

# 1 Total sulphate vs. sulphuric acid monomer in nucleation 2 studies

3

4 K. Neitola<sup>1</sup>, D. Brus<sup>1,2</sup>, U. Makkonen<sup>1</sup>, M. Sipilä<sup>3</sup>, R. L. Mauldin III<sup>3, 4</sup>, N. Sarnela<sup>3</sup>,  
5 T. Jokinen<sup>3</sup>, H. Lihavainen<sup>1</sup> and M. Kulmala<sup>3</sup>

6 [1] {Finnish Meteorological Institute, Erik Palménin aukio 1, P.O. Box 503, 00100 Helsinki,  
7 Finland}

8 [2] {Laboratory of Aerosol Chemistry and Physics, Institute of Chemical Process Fundamentals  
9 Academy of Sciences of the Czech Republic, Rozvojová 135, 165 02 Prague 6, Czech  
10 Republic}

11 [3] {Department of Physical Sciences, University of Helsinki, P.O. Box 64, 00014 Helsinki,  
12 Finland}

13 [4] {Institute for Arctic and Alpine Research, University of Colorado, Boulder, CO 80309,  
14 USA}

15 Correspondence to: K. Neitola ([kimmo.neitola@fmi.fi](mailto:kimmo.neitola@fmi.fi))

16

## 17 Abstract

18 Sulphuric acid is known to be a key component for atmospheric nucleation. Precise  
19 determination of sulphuric acid concentration is a crucial factor for prediction of nucleation  
20 rates and subsequent growth. In our study, we have noticed a substantial discrepancy between  
21 sulphuric-acid monomer and total-sulphate concentrations measured from the same source of  
22 sulphuric-acid vapour. The discrepancy of about one-to-two orders-of-magnitude was found  
23 with similar particle-formation rates. To investigate this discrepancy, and its effect on  
24 nucleation, a method of thermally controlled saturator filled with pure sulphuric acid (97 % wt.)  
25 for production of sulphuric-acid vapour is applied and rigorously tested. The saturator provided  
26 an independent vapour-production method, compared to our previous method of the furnace  
27 (Brus et al., 2010 and 2011), to find out if the discrepancy is caused by the production method  
28 itself. The saturator was used in a sulphuric acid-water nucleation experiment, using a laminar

1 flow tube to check reproducibility of the nucleation results with the saturator method, compared  
2 to the furnace. Two independent methods of mass spectrometry and online ion chromatography  
3 were used for detecting sulphuric acid or sulphate concentrations. Measured sulphuric-acid or  
4 total sulphate concentrations are compared to theoretical predictions calculated using vapour  
5 pressure and a mixing law. The calculated prediction of sulphuric-acid concentrations agrees  
6 very well with the measured values when total sulphate is considered. Sulphuric-acid monomer  
7 concentration was found to be about two orders-of-magnitude lower than theoretical  
8 predictions, but with a similar temperature dependency as the predictions and the results  
9 obtained with the ion-chromatograph method. Formation rates are reproducible when compared  
10 to our previous results with both sulphuric-acid or total-sulphate detection and sulphuric-acid  
11 production methods separately, removing any doubts that the vapour-production method would  
12 cause the discrepancy. Possible reasons for the discrepancy are discussed and some suggestions  
13 include that the missing sulphuric acid is in clusters, formed with contaminants found in most  
14 laboratory experiments. One-to-two orders-of-magnitude higher sulphuric-acid concentrations  
15 (measured as total sulphate in this study) would contribute to a higher fraction of particle growth  
16 rate than assumed from the measurements by mass spectrometers (i.e. sulphuric-acid  
17 monomer). However, the observed growth rates by sulphate-containing vapour in this study  
18 does not directly imply similar situation on field, where the sources of sulphate are much more  
19 diverse.

## 21 1 Introduction

22 Secondary particle formation by gas-to-liquid conversion is widely recognized as an important  
23 source of aerosol particles in the atmosphere worldwide (Weber et al., 1996; Kulmala et al.,  
24 2004; Spracklen et al., 2006). These particles may grow to larger sizes and affect the radiative  
25 balance of the earth by scattering and absorbing incoming radiation (Feingold and Siebert,  
26 2009). Model calculations and observations suggest that new particle formation events with  
27 subsequent growth can contribute a substantial amount to Cloud Condensation Nuclei (CCN)  
28 concentrations, which can alter the lifetime and albedo of clouds (Lihavainen et al., 2003 and  
29 2009; Merikanto et al., 2009). Furthermore, aerosols can reduce visibility and have potential  
30 health effects (Davidson et al., 2005).

31 Significant effort has been made by field measurements and laboratory studies, together with  
32 computer simulations, to understand the particle-formation mechanism itself and the

1 atmospheric conditions involved in the gas-to-liquid conversion. Despite such effort and  
2 numerous results, the underlying mechanism is not yet found.

3 It is widely accepted that sulphuric acid plays a key role in atmospheric nucleation (Kulmala et  
4 al., 2006; Sipilä et al., 2010; Brus et al., 2011; Kirkby et al., 2011). Binary nucleation of  
5 sulphuric acid and water (Vehkamäki et al., 2002; Yu, 2006; Kirkby et al., 2011), ternary  
6 nucleation involving also ammonia and/or amines (Ball et al., 1999; Korhonen et al., 1999;  
7 Napari et al., 2002; Benson et al., 2009; Berndt et al., 2010; Kirkby et al., 2011; Zollner et al.,  
8 2012) and ion-induced nucleation (Lee et al., 2003; Lovejoy et al., 2004; Yu et al., 2008, 2010;  
9 Nieminen et al., 2011) have been suggested as possible mechanisms for nucleation to occur in  
10 the atmosphere. Ions have been shown to lower the thermodynamic potential of nucleation  
11 (Arnold 1980; Winkler et al., 2008; Kirkby et al., 2011), but the role of ions in nucleation  
12 occurring in atmospheric boundary layer has been shown to be minor (Manninen et al., 2010;  
13 Paasonen, et al., 2010, Kerminen et al., 2010; Hirsikko et al., 2011).

14 Recently several laboratory studies have been conducted concerning the role of sulphuric acid  
15 in atmospheric nucleation (e.g. Benson et al., 2008, 2011; Young et al., 2008; Berndt et al.,  
16 2008, 2010; Brus et al., 2010, 2011; Sipilä et al., 2010; Kirkby et al., 2011; Zollner et al., 2012)  
17 with different methods of producing the gas phase sulphuric acid: with their own advantages  
18 and disadvantages. For example, the evaporation method of weak sulphuric-acid solution used  
19 by Viisanen et al. (1997) and Brus et al. (2010 and 2011) introduces a thermal gradient.  
20 Production of sulphuric acid with a  $\text{SO}_2 + \text{OH}$  reaction is used in most of the experiments, since  
21 it is similar to that observed in atmosphere (e.g. Benson et al., 2008; Berndt et al., 2008, 2010;  
22 Sipilä et al., 2010; Kirkby et al., 2011). The  $\text{SO}_2$  oxidation method involves the use of UV light  
23 to produce OH radicals. The excess OH must be removed so that it does not disturb the  
24 nucleation process itself (Berndt et al., 2010). Another way is to have excess  $\text{SO}_2$ , so that all  
25 the OH reacts rapidly with  $\text{SO}_2$ ; but for the calculation of the produced  $\text{H}_2\text{SO}_4$  concentration,  
26 the exact concentration of OH produced must be known (Benson et al., 2008). Ball et al., (1999)  
27 and Zollner et al., (2012) produced sulphuric acid vapour by saturating  $\text{N}_2$  flow in a glass  
28 saturator-containing pure (~96 % and ~98 %, respectively) sulphuric acid. Ball et al., (1999)  
29 varied the temperature of the saturator, whilst Zollner et al., (2012) kept the saturator at constant  
30 temperature (303 K) and varied the carrier-gas flowrate to change the sulphuric acid  
31 concentration.

1 As stated by others in literature (e.g. Benson et al., 2011; Brus et al., 2011; Kirkby et al., 2011),  
2 contaminants are present in most of the laboratory nucleation studies. These contaminants arise  
3 from different sources, such as from the water used for humidifying the carrier gas or from the  
4 carrier gas itself which contains trace levels of contaminants. It is almost impossible to remove  
5 these contaminants, which most probably affect the nucleation process itself.

6 Brus et al. (2011) reported a discrepancy in sulphuric-acid mass-balance between a known  
7 concentration of weak sulphuric-acid solution introduced to the experimental setup and a  
8 measured sulphuric-acid concentration, even though correction for wall losses and losses to  
9 particle-phase was applied, one-and-half orders-of-magnitude difference in sulphuric acid  
10 concentration was found (see Fig. 5 in Brus et al., 2011). A large discrepancy between measured  
11 sulphuric-acid monomer and total-sulphate concentration was observed in the present study too.  
12 To investigate the reason for this discrepancy, we applied a thermally controlled saturator (e.g.  
13 Wyslouzil et al., 1991; Ball et al., 1999) to produce sulphuric-acid vapour. The output of the  
14 saturator was tested with two independent detection methods (mass spectrometry and ion  
15 chromatography) before using the saturator in a sulphuric acid-water nucleation study in a  
16 laminar flow tube.

17 Applying the saturator as the source of the sulphuric-acid vapour made it possible to compare  
18 the saturator to the furnace, which was used as the source of the sulphuric acid previously (Brus  
19 et al., 2010 and 2011) and eliminate the production method as a reason for the discrepancy. The  
20 flow-tube measurements with the saturator and the two sulphuric-acid or total-sulphate  
21 detection methods were conducted to check reproducibility of particle formation rates between  
22 the saturator and the furnace, with similar observed sulphuric-acid or total-sulphate  
23 concentrations. The measured sulphuric-acid or total-sulphate concentrations were compared  
24 and the total losses of sulphuric acid or sulphate were determined for both mass spectrometers  
25 and the ion chromatograph. The level of ammonia contaminant in the system was determined  
26 with the ion-chromatograph method.

27 Introducing saturator as the source of sulphuric acid vapour reduces disadvantages associated  
28 with other methods, like a temperature gradient arising from usage of furnace, or calculations  
29 of OH concentration produced with UV light and removal of excess OH associated with the  
30 oxidation of SO<sub>2</sub>. The major disadvantage using this method is the handling of pure sulphuric  
31 acid when filling the saturator. Luckily, the saturation vapour pressure of sulphuric acid is very  
32 low and therefore, the sulphuric acid is consumed very slowly. Due to the high hygroscopicity

1 of sulphuric acid, the saturator should not be exposed to humid flow as the pure liquid sulphuric  
2 acid would draw water vapour from the flow contaminating the sulphuric acid. This would lead  
3 to a significant error in the predicted concentration due to a much higher vapour pressure of  
4 water compared to sulphuric acid.

## 6 2 Experimental

7 The measurement setup presented here is partially introduced in Brus et al. (2010), and only the  
8 main principle of the method and the most substantial changes are described here. The setup  
9 for testing the output of the saturator with two independent sulphuric-acid or total-sulphate  
10 detection methods is described. The instrumentation for sulphuric-acid or total-sulphate and  
11 freshly-formed-particle detection is shortly presented.

### 12 2.1 Saturator

13 The saturator was a horizontally placed cylinder made of iron with Teflon insert inside the  
14 cylinder (inner diameter, I.D., of 5 cm). It was thermally controlled with a liquid-circulating  
15 bath (LAUDA RC 6) and the temperature was measured just above the liquid surface with a  
16 calibrated PT100 probe (accuracy  $\pm 0.05$  K) inserted from the outlet side of the saturator (Fig.  
17 1). The saturator was filled with 150-200 ml of pure sulphuric acid (~97 % wt., Baker analyzed).  
18 H<sub>2</sub>SO<sub>4</sub> vapour was produced by flowing purified, dry, particle-free carrier gas through the  
19 saturator in the range of 0.05-1 litres per minute (lpm) saturating the flow with vapour according  
20 to the temperature of the saturator. Carrier gas flows were purified in all experiments first with  
21 activated carbon capsules (Pall Corp., USA) to remove all organic vapours via diffusion to the  
22 surfaces and after with a HEPA filters (Pall Corp. USA) to remove any particles left in the flow.  
23 The saturator flow was thermally controlled to the same temperature as the saturator before  
24 entering it, to ensure temperature stability inside the saturator.

25 The theoretical prediction of sulphuric-acid vapour concentration was calculated using the  
26 equation for vapour pressure from Kulmala and Laaksonen (1990) which uses the  
27 measurements by Ayers et al. (1980) and theoretically extrapolates the vapour pressure to lower  
28 range of temperatures used in this study:

$$29 \ln p = \ln p_0 + \frac{\Delta H_v(T_0)}{R} \times \left[ -\frac{1}{T} + \frac{1}{T_0} + \frac{0.38}{T_c - T_0} \times \left( 1 + \ln \frac{T_0}{T} - \frac{T_0}{T} \right) \right], \quad (1)$$

1 where  $p$  is the vapour pressure (atm),  $p_0 = - (10156 / T_0) + 16.259$  atm (Ayers et al., 1980),  $T$  is  
2 the temperature,  $T_c$  is critical temperature, 905 K, and  $T_0$  is chosen to be 360 K so  $\Delta H_v (T_0) / R$   
3 = 10156. See Kulmala and Laaksonen (1990) for more details. Here the predicted sulphuric-  
4 acid concentration depends only on saturator temperature, flowrate through the saturator and  
5 mixing flow. Measured sulphuric-acid or total-sulphate concentration is compared also to  
6 empirical fit by Richardson et al. (1986):

$$7 \quad \ln p = 20.70 - \frac{9360}{T} . \quad (2)$$

8 The fit is made to their measurement data in the temperature range of 263.15-303.15 K, which  
9 suits the temperature range of the present study.

## 10 **2.2 Setup for testing saturator with mass spectrometers and online ion** 11 **chromatograph**

12 The saturator was tested in two different tests. First with mass spectrometers: Chemical  
13 Ionization Mass Spectrometer (CIMS) (Eisele and Tanner, 1993; Mauldin et al., 1998; Petäjä  
14 et al., 2009) and Atmospheric Pressure interface Time Of Flight mass spectrometer, (CI-Api-  
15 TOF, Tofwerk AG, Thun, Switzerland and Aerodyne Research Inc., USA; Junninen et al.,  
16 2010) with a similar Chemical Ionization inlet as the CIMS (Jokinen et al., 2012). A second test  
17 was done with the instrument for Measuring AeRosols and GAses (MARGA, Metrohm  
18 Applikon Analytical BV, Netherlands; ten Brink et al., 2007). Both measurements were  
19 performed with the same setup (Fig. 1). The flow from the saturator (0.5 lpm) was mixed with  
20 another flow of the same gas (20 or 40 lpm) after the saturator to meet the inlet flows of the  
21 instruments. The relative humidity (RH) was set by 2 or 3 Nafion humidifiers (MD-series,  
22 Perma pure, USA) and monitored from the excess flow. The design of the inlet system for  
23 mixing the different flows and flow schematics to the instruments can be found in the  
24 supplementary material (Fig. S2). Different configurations after the mixing were tested and no  
25 difference in the observed concentration was found. The temperature of the saturator was  
26 increased in 5-degree steps from approximately 273 K to 303 K (MARGA) and 313 K (CIMS  
27 and CI-Api-TOF) in order to increase the sulphuric-acid concentration. The temperature was  
28 kept constant from 2 to 8 hours in order to achieve a steady state. The measured sulphuric-acid  
29 monomer and total-sulphate concentrations were compared to theoretical values calculated  
30 from the vapour pressure of sulphuric acid using Eq. (1) and (2).

### 1 **2.3 Flow-tube setup for nucleation measurements**

2 The flow-tube setup consists of four main parts: a saturator, a mixing unit, a flow nucleation  
3 chamber and detection of sulphuric acid or total sulphate and particles (Fig. 2). The sulphuric-  
4 acid vapour is produced in the saturator and turbulently mixed with clean, particle-free carrier  
5 gas in the mixing unit. Particles formed inside the saturator are lost in the 1-m long, thermally  
6 controlled Teflon tube (I.D. 4 mm) before the mixer, by diffusion and by the turbulent mixing  
7 in the mixer. After the mixing unit, nucleation and subsequent growth take place in the laminar  
8 flow chamber. The flow chamber consists of two 100-cm-long stainless steel cylinders (I.D. 6  
9 cm) connected with a Teflon piece (height 3.5 cm, I.D. 6 cm), positioned vertically and  
10 thermally controlled with a liquid circulating bath (LAUDA RC 6). One of the 100-cm-long  
11 parts of the flow chamber has four holes on the sides every 20 cm from the beginning of the  
12 chamber. The 3.5-cm Teflon connector between the two 100-cm flow-tube pieces has also a  
13 hole (see Fig. 2). These holes are used to continuously measure temperature in the flow tube  
14 with PT100 probes to ensure constant desired nucleation temperature. The RH of the mixing  
15 flow is controlled by 2 or 3 Nafion humidifiers. RH and temperature are measured also at the  
16 end of the tube with Vaisala HMP37E and humidity data processor Vaisala HMI38. Both  
17 saturator and mixing flow of the tube are controlled by a mass flowrate controller (MKS type  
18 250) with an accuracy of  $\pm 3\%$ . Flowrates through the saturator for nucleation measurements  
19 were kept at 0.13-0.27 lpm. The mixing flow was kept at approximately 11 lpm.

### 20 **2.4 H<sub>2</sub>SO<sub>4</sub> monomer, sulphate and particle detection**

21 Gas phase sulphuric-acid monomers were measured with CIMS or CI-API-TOF. The CI-inlet  
22 used in both instruments works as follows: the sulphuric-acid molecules are ionized in ambient  
23 pressure via proton transfer between nitrate ions (NO<sub>3</sub><sup>-</sup>) and sulphuric acid molecules (H<sub>2</sub>SO<sub>4</sub>).  
24 The nitrate ions are produced from nitric acid with radioactive <sup>241</sup>Am-source and mixed in a  
25 controlled manner in a drift tube, using a concentric sheath and sample flows together with  
26 electrostatic lenses.

27 After the ionization in the inlet, the instruments differ from each other. In the CIMS sample,  
28 flow is dried using a nitrogen flow to dehydrate the molecules before entering the vacuum  
29 system and [detection in the quadrupole mass spectrometer. In the CI-API-TOF, a flowrate of](#)  
30 [0.8 lpm is guided through a critical orifice. The ions are guided through the differentially](#)

1 pumped Atmospheric pressure interface (Api) and finally to the TOF for detection according to  
2 the ions' mass-to-charge ratio.

3 The monomer concentration is determined by the ratio of the resulting ion signals ( $\text{HSO}_4^-$  and  
4  $\text{HSO}_4^- \cdot \text{HNO}_3$ ) and the reagent ion signals ( $\text{NO}_3^-$ ,  $\text{HNO}_3 \cdot \text{NO}_3^-$  and  $(\text{HNO}_3)_2 \cdot \text{NO}_3^-$ ). This ratio is  
5 then multiplied by the instrument-dependent calibration factor in both instruments. The  
6 calibration factor used here was  $5 \cdot 10^9$  for both instruments. Neither CIMS nor CI-Api-TOF was  
7 calibrated using the saturator setup, but instead before the experiments using the standard  
8 calibration procedure of oxidation of  $\text{SO}_2$  with OH (Kürten et al., 2012). For more information  
9 about the calibration of CIMS, see Berresheim et al. (2000), Petäjä et al. (2009), Zheng et al.  
10 (2010) and Kürten et al. (2012). The nominal sample flowrate of these instruments is  $\sim 10$  lpm.  
11 We considered only the monomer concentration, although detection of dimers and even larger  
12 clusters of pure sulphuric acid is possible with CI-Api-TOF. This was done because the dimer  
13 concentration was always in the magnitude of  $\sim 1$  % of monomer concentration and the trimer  
14 concentration was in the magnitude of  $\sim 1$  % of the dimer concentration and so on (e.g. Jokinen  
15 et al. 2012). The charging efficiency might not be the same for these clusters as it is for  
16 monomer. This would cause the calibration factor to change and the calculated concentration  
17 to be erroneous. The uncertainty in the resulting monomer concentration is estimated to be a  
18 factor of  $\sim 2$ . The nominal lower detection limit of CIMS and CI-Api-TOF is estimated to be  
19  $5 \cdot 10^4 \text{ cm}^{-3}$ , and the upper limit is approximately  $10^9 \text{ cm}^{-3}$  for both instruments. At this high  
20 concentration, the primary ions start to deplete causing the calibration factor to change.

21 The total sulphate concentration was measured with an online ion chromatograph MARGA 2S  
22 ADI 2080. MARGA is able to detect 5 gases in the gas phase ( $\text{HCl}$ ,  $\text{HNO}_3$ ,  $\text{HONO}$ ,  $\text{NH}_3$ ,  $\text{SO}_2$ )  
23 and 8 major inorganic species in aerosol phase ( $\text{Cl}^-$ ,  $\text{NO}_3^-$ ,  $\text{SO}_4^{2-}$ ,  $\text{NH}_4^+$ ,  $\text{Na}^+$ ,  $\text{K}^+$ ,  $\text{Mg}^{2+}$ ,  $\text{Ca}^{2+}$ ).  
24 The sample flow is  $\sim 16.7$  lpm. From the sample flow, all (more than 99.7 %) of water-soluble  
25 gases are absorbed into a wetted rotating denuder (WRD). Based on different diffusion  
26 velocities, aerosols pass the WRD and enter a Steam-Jet-Aerosol-Collector (SJAC) (Slanina et  
27 al., 2001). In the SJAC, conditions are supersaturated with water vapour, which condenses onto  
28 particles and the particles thus collect at the bottom of the SJAC. Sample solutions are drawn  
29 from the WRD and the SJAC into syringes (25 ml) and are analysed one after another once an  
30 hour. Samples are injected in cation and anion chromatographs with an internal standard (LiBr).  
31 Components are detected by conductivity measurements. The detection limits are  $0.1 \mu\text{g m}^{-3}$  or  
32 better. For more information about the instrument, see Makkonen et al. (2012).



1 In our previous study (Brus et al., 2010), the total sulphate concentration was measured using  
2 the method of bubblers: where a known flowrate from the flow tube was bubbled through  
3 alkaline solution, thus trapping sulphate. This solution was then analysed using offline ion  
4 chromatography. See Brus et al., (2010) for details. The method of bubbler is analogous to the  
5 MARGA and the main difference is that MARGA is an online method, whilst bubbler is an  
6 offline method.

7 The total-particle number concentration was measured with a Particle Size Magnifier (PSM,  
8 Airmodus Oy, Finland, Vanhanen et al., 2011, coupled with CPC TSI model 3772) and with  
9 Ultra-Fine CPC's (UFCPC, TSI models 3776, 3025A) with cut-off mobility diameters of ~1.5  
10 nm and ~3 nm, respectively. Differential Mobility Particle Sizer (DMPS) was used to measure  
11 particle number size distribution from 3 to ~250 nm in a closed-loop arrangement (Jokinen and  
12 Mäkelä, 1997) using a blower to measure the wet size of the particles. The DMPS was run with  
13 a sheath flow of ~11 lpm and sample flow of 1.5 lpm in the short HAUKE-type Differential  
14 Mobility Analyzer (DMA). The DMA was coupled with UFCPC (TSI model 3025A) and with  
15 a bipolar radioactive (<sup>63</sup>Ni) neutralizer. The charging efficiencies were calculated following the  
16 parameterization of Wiedensohler and Fissan (1991). The RH of the sheath flow was monitored  
17 to ensure that it was same as the RH in the chamber.

18

### 19 **3 Results**

20 To quantify the sulphuric acid input for flow-tube nucleation measurements, the saturator  
21 output was tested in two experiments: first with CIMS and CI-API-TOF and second with  
22 MARGA. After the tests, nucleation measurements of sulphuric acid-water system were  
23 conducted. This enabled direct comparison with the sulphuric-acid production method used in  
24 our previous studies (Brus et al., 2010 and 2011), so that the production method can be  
25 discounted as a reason for the discrepancy. Presented values from CIMS, CI-API-TOF and  
26 MARGA measurements are residual, i.e. measured values at the end of the flow tube accounting  
27 for dilutions, if not otherwise mentioned to be different.

#### 28 **3.1 Test of the saturator**

29 Results of the saturator test are presented in Fig. 3 as measured sulphuric-acid or total-sulphate  
30 concentrations and predicted values by Eq. (1) and (2) as a function of temperature of the  
31 saturator. The mixing flows were 40 (dry and RH 15 %) or 20 lpm (for RH 29 %) for CIMS

1 and Api-TOF and 20 lpm (only dry conditions) for MARGA measurements. Tests with  
2 MARGA were performed with dry conditions, since it was noticed that the RH did not have  
3 any influence on the results from the tests with mass spectrometers. MARGA uses  
4 supersaturated conditions to grow the particles and collect them in the SJAC, hence initial RH  
5 is not expected to have any influence. Saturator flowrate was 0.5 lpm. Mass spectrometers were  
6 tested in dry and humid conditions. Dry experiments were run with two mass-spectrometer inlet  
7 flowrates (6 and 10 lpm) and with extra 1 m (I.D. 4 mm) Teflon tubing between the saturator  
8 and the mixing unit, to test the effect of wall losses. Humidified experiments were done with  
9 two inlet flowrates (6 lpm for RH 29 % and 10 lpm for RH 15 %). MARGA experiments were  
10 conducted in dry conditions.

11 The total sulphate concentration measured with MARGA (black squares) fits the prediction by  
12 Eq. (2) (dashed line) very well and the prediction by Eq. (1) (solid line) underestimates the  
13 measured total sulphate concentration slightly. MARGA has a relatively fast inlet flowrate  
14 (~16.7 lpm) so inlet losses are low; however, with increased temperature of the saturator,  
15 diffusional losses are visible.

16 Sulphuric-acid monomer concentration measured with CIMS and CI-Api-TOF fit each other  
17 very well, but they show one-to-two orders-of-magnitude lower concentrations than predicted  
18 by Eq. (1) and (2) and measured total sulphate with MARGA. The slope is similar to the  
19 predictions and to the points measured with MARGA. The dimer concentration was always  
20 approximately 1 to 10 % (increasing with increasing saturator temperature) of the monomer  
21 concentration and trimer approximately 1 % of the dimer concentration (see supplementary  
22 material, Fig. S5).

23 Relative humidity did not have any substantial effect on the measured values by CIMS and CI-  
24 Api-TOF. RH can affect the wall losses by preventing the sulphuric acid's evaporation from  
25 the inlet walls, since the vapour pressure of water is several orders of magnitude higher than  
26 that of the sulphuric acid. The predictions by Eq. (1) and (2) do not consider relative humidity,  
27 since the flow through the saturator is always dry. The relative humidity of the mixing flow  
28 causes the sulphuric acid molecules to get hydrated since sulphuric acid is very hygroscopic;  
29 but because the results from humid and dry measurements are very similar, CIMS and CI-Api-  
30 TOF can be considered to measure well in humid conditions also. The effect of RH is discussed  
31 in Eisele and Tanner (1995) and our results agree with the discussion there.

1 A change of the nominal inlet flowrate of CIMS and CI-API-TOF did not have large effect. The  
2 inlet lines were short (~20 cm) in the saturator tests so the wall losses due to lower inlet flowrate  
3 did not play any significant role. Using instruments with a lower flowrate might alter the  
4 measured concentration as the calibration factor is acquired with inlet flowrate of 10 lpm.

5 Tests with different saturator flow rates (0.05 - 1 lpm) were conducted to estimate the limits of  
6 the saturator flow (not shown in Fig. 3). With 0.05 lpm saturator flow rate diffusional losses to  
7 the walls dominated causing the measured sulphuric acid concentrations decrease as a function  
8 of the saturator temperature. In the saturator flow rate range from 0.2 up to at least 1 lpm,  
9 sulphuric acid concentrations behaved as expected. Results of different flow rate tests, as well  
10 as results from tests with carrier gases with different purity, can be found in the supplementary  
11 material (sections 3 and 4).

12 Extra saturator tests with mass spectrometers were done using three different carrier gas purities  
13 ( $N_2$  6.0,  $N_2$  5.0 and pressurized air) to check if the carrier gas used in our experiments  
14 (pressurized air) was more dirty than the most pure commercial ones. Two different purity  
15 sulphuric acids (~97 % and 100 %) were tested also to check if the purity of the acid itself has  
16 an influence. Changing the carrier gas or the sulphuric acid purity did not affect the observed  
17 sulphuric-acid concentration (see supplementary material, Fig. S3 and S4). The measured  
18 sulphuric-acid monomer concentration was one-to-two orders-of-magnitude lower than the  
19 prediction by Eq. 1. Tests with different saturator flowrates (0.05-2 lpm) showed that with  
20 flowrates below 0.1 lpm, diffusion losses dominated: causing the measured concentration to  
21 decrease as a function of the saturator flowrate. Above 0.15 lpm, the observed results behaved  
22 as expected. The measured cluster distributions (monomer, dimer and trimer) with different  
23 carrier gas purity were constant through the measured saturator flowrate range (Fig. S5). The  
24 ratios between monomer-to-dimer and dimer-to-trimer were between 1:10 and 1:100 with all  
25 carrier gases. From these results it is evident that the carrier gas used in our studies does not  
26 contain more contaminants than the most pure ones commercially available. CI-API-TOF mass  
27 spectra observed with different carrier gases were investigated further to find the missing  
28 sulphuric acid. A large number of peaks were found to correlate with mass 97 ( $HSO_4^-$ ), which  
29 is the ionized sulphuric-acid monomer, with all carrier gases. The number of these peaks  
30 increased as a function of the saturator temperature, suggestive that the sulphuric acid forms  
31 clusters with contaminant substances (Supplementary, section 6, Fig. S6-S8). The correlating  
32 peaks in Fig. S6-S8 are stick masses (i.e. rounded to nearest integer), which means that many

1 of those peaks have actually several peaks within them. This is shown in Fig. S9-S11 where the  
2 mass spectrum from CI-API-TOF is zoomed in. Unfortunately, summing up all of these  
3 correlating peaks to calculate the total sulphuric acid concentration is not feasible, since these  
4 clusters are not identified (i.e. it is not known what molecules those clusters are composed of)  
5 and the sheer number of these peaks is overwhelming. For more details and discussion of the  
6 extra saturator tests, see supplementary material.

### 7 **3.2 Losses of sulphuric acid and sulphate in the flow tube**

8 Total losses were not directly measured but they were determined by comparing results from  
9 saturator tests with the results from nucleation measurements. The setup of the measurements  
10 was similar in both experiments except for the flow tube used in nucleation measurements. By  
11 accounting for the different mixing ratios of saturator flowrate and mixing flowrate, these  
12 measurements become comparable and the total losses in the flow tube can be determined. The  
13 Total Loss Factor (*TLF*) includes wall losses and losses to the particle phase (nucleation and  
14 condensational losses).

15 Figure 4 presents the measured sulphuric-acid-monomer and total-sulphate concentration from  
16 the saturator tests (squares) and nucleation measurements (stars) as a function of the saturator  
17 temperature. Saturator tests were done in dry conditions and nucleation measurements in RH  
18 30 %. An inlet pipe is used to connect the mass spectrometer to the flow tube. Brus et al. (2011)  
19 state that the Wall Loss Factor (*WLF*) in the inlet pipe of length 100 + 22 cm is  $WLF_{\text{inlet}} = \sim 4$ .  
20 This factor, together with the mixing ratios, was accounted for to make the data sets directly  
21 comparable.

22 A linear fit was applied to the data and *TLF* values were determined from the ratio of the fits.  
23 The *TLF* values were determined for a saturator temperature range of 286-300 K for CIMS and  
24 284-297 K for MARGA depending on the measurement range of the data. The average *TLF*  
25 values are  $14.2 \pm 4.2$  for CIMS and  $10.0 \pm 1.2$  for MARGA. The  $R^2$  values for the fits are 0.96,  
26 0.87, 0.90 and 0.61 for CIMS saturator test, CIMS nucleation measurement, MARGA saturator  
27 test and MARGA nucleation measurement, respectively.

28 From Fig. 4, it is evident that wall losses are not the only losses affecting the measured  
29 concentrations since the trends in the fits for nucleation measurements are less steep than the  
30 ones from saturator tests. The losses to the particle phase also affect the situation. The maximum  
31 losses of sulphuric acid to particle phase are calculated using the DMPS data measured at the

1 end of the nucleation chamber only. The total volume of the particles is calculated within the  
2 size distribution assuming that the particles are composed only of pure sulphuric acid with  
3 density of  $1.84 \text{ g cm}^{-3}$ . The losses of sulphuric acid to particles range from 0 % (dry conditions,  
4  $T_{\text{sat}} = 273 \text{ K}$ ) up to maximum of 1.4 % (RH = 30 %,  $T_{\text{sat}} = 292 \text{ K}$ ) of the total sulphate  
5 concentration. Higher saturator temperature increases the number and the diameter of the  
6 particles, and relative humidity increases the diameter of the particles. The losses to the particle  
7 phase are substantial at the highest values of saturator temperature but this estimate is the  
8 maximum limit since the particles are not composed only of pure sulphuric-acid molecules.  
9 Contaminants from the flow condense to the particle phase or bond with sulphuric acid. When  
10 using humid conditions, sulphuric-acid particles uptake water since sulphuric acid is very  
11 hygroscopic. At the highest temperature of the saturator, the size distribution unfortunately  
12 extends out of the DMPS range (3-250 nm), thus conversely underestimating the losses. Losses  
13 to the clusters smaller than the cut-off size of the particle counters are **substantial**. **The**  
14 **maximum losses to the particle phase have been calculated for each of the saturator temperature**  
15 **values and plotted with the measured monomer and total sulphate concentrations together with**  
16 **the prediction from Eq. (1) in Fig. S1 in supplementary material. Even summing up the**  
17 **measured monomer concentration and the losses to the particle phase leaves the summed total**  
18 **concentration at least one order of magnitude lower than the measured total sulphate and the**  
19 **prediction by Eq. (1).**

### 20 **3.3 Nucleation measurements**

21 Formation rates  $J$  of sulphuric acid-water were measured in the range from 0.1 to  $\sim 300 \text{ cm}^{-3}\text{s}^{-1}$   
22 with sulphuric acid monomer concentration approximately from  $5 \cdot 10^5$  to  $10^7 \text{ cm}^{-3}$  or in total  
23 sulphate concentration approximately from  $4 \cdot 10^8$  to  $3 \cdot 10^9 \text{ cm}^{-3}$ . Formation rates are usually  
24 reported as  $J_{1.5}$  or  $J_3$  (cut-off sizes of the particle counters are 1.5 nm for PSM and 3 nm for  
25 UFCPC TSI models 3776 and 3025) as discussed in Kulmala et al. (2012). However, particles  
26 measured at the end of our flow tube were almost always in the range of 8-20 nm, so we report  
27 formation rates as they were determined with our particle counters. **The purpose of these**  
28 **nucleation measurements is to be able to compare the formation rates and the sulphuric-acid or**  
29 **total-sulphate concentrations, between the two sulphuric-acid vapour-production methods.** The  
30 results are discussed below.

31 Figure 5 presents DMPS and CIMS data for one cycle of saturator temperatures. Panel a)  
32 presents the number size distribution as a function of time, panel b) the total particle number

1 concentration, panel c) shows the hourly averaged sulphuric-acid monomer concentration with  
2 standard deviation as the error bars and panel d) shows hourly averaged saturator temperature.  
3 One can see from Fig. 5, panels a) and b), that when the temperature of the saturator changes,  
4 the number concentration and the number size distribution are not stable immediately. The  
5 sulphuric-acid concentration overshoots slightly at the beginning whilst the system stabilizes to  
6 steady state. The first hour of averages from each of the saturator temperatures was excluded  
7 to ensure only steady-state data ( $\text{std}(T) = \pm 0.05 \text{ K}$ ) were included in the averages. When a new  
8 cycle started, the  $T_{\text{sat}}$  dropped from the maximum value ( $\sim 315 \text{ K}$ ) to the minimum ( $273 \text{ K}$ )  
9 causing a long period of unstable data, and the first two hours were excluded from the beginning  
10 of the cycle. In panel a) in Fig. 5, nucleation is the main process below temperature of  $\sim 290 \text{ K}$   
11 and growth takes over at higher temperatures. This can be seen as the bimodal distribution at  
12 highest saturator temperatures.

13 Figures 6 and 7 present the number concentration  $N_{\text{exp}}$  (panel a)), geometric mean diameter  $D_p$   
14 (panel b)) and apparent formation rate  $J$  (panel c)) of freshly nucleated particles with sulphuric-  
15 acid monomer concentration [ $\text{H}_2\text{SO}_4$  monomer] or total sulphate [ $\text{SO}_4^{2-}$ ] (panel d)) as a function  
16 of saturator temperature  $T_{\text{sat}}$  for nucleation temperature of  $298 \text{ K}$  with several different relative  
17 humidity values (Fig. 6) and saturator flowrates (Fig. 7). The formation rate is reported the  
18 observed particle concentration  $N_{\text{exp}}$  divided by the residence time  $\tau$ .

19 From Fig. 6, it is evident that all measured variables behave as expected as a function of the  
20 saturator temperature, except for the apparent saturation of the observed particle concentration  
21 (and hence, the formation rate). PSM was coupled with the TSI model 3772 CPC's, which has  
22 an upper limit of  $10^4 \text{ cm}^{-3}$  for the particle concentration. This caused the observed particle  
23 concentration to saturate in Fig. 6, even though the particle concentration was confirmed to  
24 increase to higher values by DMPS data (not shown in the Fig. 6). Coagulation has a minor  
25 effect on the particle number due to a short residence time ( $\tau = 30 \text{ s}$ ) and relatively low particle  
26 concentration. The relative humidity affects mostly the diameter of the particles, but also  
27 decreasing RH decreases the formation rate if similar sulphuric acid concentration is  
28 considered. A lower formation rate with decreased RH might be caused by the diminishing of  
29 the particle diameter below the detection limit of the UFCPC (TSI model 3776). In Fig. 7, the  
30 squares present measurements during dry conditions and stars during RH of 30 %. Panel d)  
31 shows also the detection limit of MARGA for total sulphate concentration. The detection limit  
32 was determined from 20 hours of measurements with saturator flowrate set to zero and averaged

1 over the time period. The detection limit was  $1.35 \cdot 10^9 \text{ cm}^{-3}$ . All the total sulphate concentrations  
2 measured below this detection limit were considered as erroneous and rejected from further  
3 analysis, even though these values are presented in Fig. 7. MARGA can be used with  
4 concentration columns to measure lower concentrations of species but it was not available in  
5 this study.

6 From Fig. 7, one can see that all the variables responded in a similar manner as CIMS and CI-  
7 Api-TOF experiment (Fig. 6). As the temperature of the saturator approaches the temperature  
8 of the mixing unit (laboratory temperature,  $\sim 294 \text{ K}$ ) the number concentration of particles  
9 decreases and starts to increase again when saturator temperature is greater than that of the  
10 mixing unit. This is an artefact of the setup.

11 The main difference between Fig. 6 and 7 is the maximum diameter reached. Due to the greater  
12 maximum saturator temperature ( $315 \text{ K}$ ) in the experiment with the mass spectrometers, the  
13 maximum diameter reached up to  $\sim 130 \text{ nm}$  compared to the  $\sim 23 \text{ nm}$  with the experiment with  
14 MARGA. The residence times in the flow tube are the same in both experiments ( $\sim 30 \text{ s}$ ). The  
15 measured sulphuric-acid monomer concentration is at typical atmospheric levels, but the  
16 growth rates are much higher: indicating higher concentration of sulphuric-acid-containing  
17 condensing vapour than the detected sulphuric-acid-monomer concentration by CIMS. The  
18 growth is rather driven by the total sulphate, originating exclusively from the sulphuric acid  
19 inside the saturator, than the sulphuric-acid-monomer concentration.

20 To show the contribution of the sulphate to the growth rate, the model described in Škrabalová  
21 et al. (2014) was used to calculate the diameter ( $D_p$ ) and growth rate ( $GR$ ) of the particles.  
22 Measured sulphuric-acid monomer and total-sulphate concentrations (Fig. 6 and 7, panel d),  
23 RH 30 %) were multiplied by the  $TLFs$  to obtain the initial concentrations of vapour at the  
24 beginning of the flow tube. Diameter of  $1.5 \text{ nm}$  was chosen as the initial cluster size according  
25 to Kulmala et al. (2007). The model was used with three scenarios of particle neutralization by  
26 ammonia: (0) no neutralization, particles composed of sulphuric acid and water, (1)  
27 neutralization to ammonium bisulphate-water particles and (2) neutralization to ammonium  
28 sulphate-water particles. When accounting for the initial sulphuric-acid monomer concentration  
29 as an input, the resulting diameter ( $D_p$ ) was always below  $2 \text{ nm}$  with growth rates ( $GR$ ) ranging  
30 approximately from  $1$  to  $15 \text{ nm h}^{-1}$  as a function of the sulphuric-acid concentration (i.e.  
31 saturator temperature  $T_{sat}$ ) with all scenarios. When total-sulphate concentration was used as an

1 input, the resulting particle diameters and growth rates fit well with the measured particle  
2 diameters presented in Fig. 7 for all scenarios (see suppl. Material, section 7 and Fig. S12).

### 3 **3.4 Formation rates and comparison to our previous results**

4 Figure 8 presents formation rates  $J$  of the  $\text{H}_2\text{SO}_4\text{-H}_2\text{O}$  system as a function of sulphuric-acid  
5 monomer concentration measured with CIMS at nucleation temperature of  $T = 298$  K and RH  
6 of  $\sim 30$  %. Sulphuric acid was produced with the method of furnace (red squares, Brus et al.,  
7 2011) and with saturator (the black squares, present study). The sulphuric-acid concentration  
8 for data from Brus et al. (2011) is presented here as residual concentration (i.e. at the end of the  
9 flow tube) so that these two measurements would be comparable. Brus et al. (2011) present  
10 their data as the initial concentration. Both datasets have almost identical slopes (1.3 and 1.2)  
11 and the formation rates  $J$  have a difference of a factor of 2. For the dataset measured with the  
12 production method of the furnace, the residence time ( $\tau = 15$  s) is defined as the time that the  
13 particles spend in the flow tube after the nucleation zone. The nucleation zone was  
14 experimentally determined (Brus et al., 2010) and confirmed with CFD model (Herrmann et  
15 al., 2010) to be in the middle of the flow tube in the measurements with the furnace, where a  
16 thermal gradient was present. For the saturator measurements (present work), the residence time  
17 ( $\tau = 30$  s) was defined as the whole time the particles spend in the flow tube. The difference of  
18 the residence time is exactly a factor of 2. Formation rate is defined as the number concentration  
19 divided by the residence time, so these two sets of data lie on top of each other if the same  
20 residence time would have been used for formation-rate determination.

21 Figure 9 presents formation rates  $J$  of  $\text{H}_2\text{SO}_4\text{-H}_2\text{O}$  as a function of residual total sulphate  
22 concentration  $[\text{SO}_4^{2-}]$  at RH of  $\sim 30$  % and at nucleation temperature of  $T = 298$  K. Stars are the  
23 data from measurements where sulphuric-acid vapour was produced with the furnace and total  
24 sulphate measured with bubbler method (Brus et al., 2010). The residence time used in there  
25 was  $\tau = 15$  s. Squares are total sulphate measured with MARGA in this study with different  
26 flowrates through the saturator, and the residence time was  $\tau = 30$  s. All the points have the  
27 standard deviation as error bars. The detection limit of MARGA is also marked as a dashed  
28 vertical line. Formation rates are similar with both production methods. As previously, the  
29 factor of two difference in the residence time increases the scatter between the two datasets.

30 Figures 8 and 9 show that apparent formation rates are reproducible with both sulphuric-acid  
31 production methods, with similar observed sulphuric-acid or total-sulphate concentrations. This



1 eliminates the sulphuric-acid production method as a reason for the discrepancy between the  
2 measured monomer and total sulphate concentrations. The data are more scattered in Fig. 9 due  
3 to the larger integration times used in MARGA and bubbler measurements. During several  
4 hours of integration time, a small change in flowrates can cause a substantial difference in the  
5 resulting concentration. MARGA data are close to the detection limit of the instrument, which  
6 also causes larger scatter.

7 Figure 10 shows comparison of the apparent formation rates  $J$  as a function of residual  
8 sulphuric-acid monomer [ $\text{H}_2\text{SO}_4$  monomer] or total sulphate concentration [ $\text{SO}_4^{2-}$ ] from this  
9 study to our previous studies with the standard deviation as error bars. Note the difference of a  
10 factor of two between the residence times. Squares show values measured using mass  
11 spectrometers (PSM, red and black squares; TSI 3776, green squares). Stars are data measured  
12 using ion-chromatograph (i.e. total sulphate) methods with two different UFCPC's (TSI 3025A,  
13 black stars and TSI 3776, red stars). Figure 10 shows that the production method does not have  
14 substantial effect since the results lie on same line when comparing results obtained with mass  
15 spectrometers or MARGA and bubbler method. The conditions for all the measurements were  
16 similar ( $T = 298 \text{ K}$ ,  $\text{RH} \sim 30 \%$ ).

17 The slope of the data measured using MARGA or bubblers is steeper than the slope of the  
18 results measured with mass spectrometers. There is a discrepancy of one-to-two orders-of-  
19 magnitude between sulphuric-acid monomer and total-sulphate concentration for similar  
20 formation rates. The UFCPC 3776 (green squares) was probably undercounting at the lowest  
21 sulphuric acid concentrations. This can be seen in Fig. 10 where the lowest observed formation  
22 rates are not consistent with the rest of the data. This is probably caused by the small size of the  
23 particles at such low sulphuric-acid concentration ( $1\text{-}2 \cdot 10^6 \text{ cm}^{-3}$ ) (Sipilä et al., 2010).

24 The comparison to literature data was omitted in this manuscript as the formation rates in the  
25 present study are very similar to our previous results (Brus et al., 2010 and 2011). However, for  
26 comparison and review of experimental data on sulphuric-acid nucleation, we refer to Zollner  
27 et al., (2012) and Zhang et al., (2012).

### 28 3.5 Contaminants

29 In our previous study (Brus et al., 2011), an ion chromatograph was used to determine the  
30 background levels of ammonia and it was found that the background concentration was below  
31 the detection limit of the IC (500 pptv), accounting for the flowrates in the nucleation chamber.

1 The concentration of background ammonia was measured with the MARGA system in this  
2 study. An average total concentration (gas and particle phase) of ammonia was 60 pptv for dry  
3 conditions and 126 pptv for RH 30 %, supporting our previous results. The concentration did  
4 not change as a function of saturator temperature, thus it is assumed to originate from the  
5 purified, particle-free air used as carrier gas in all measurements and the ultrapure water (Milli-  
6 Q, Millipore) used for humidification. The concentration for dry conditions is in the same order  
7 of magnitude as the concentration of total sulphate at the lowest (273 K) temperature of the  
8 saturator. When increasing the saturator temperature, ammonia to total sulphate-ratio decreases  
9 from ~1:1 to ~1:10 or less for dry conditions and from ~3:1 to ~1:5 for humid conditions.

10 **Results of extensive measurements and discussion of the influence of several different carrier**  
11 **gases on measured sulphuric acid concentration by mass spectrometers can be found in the**  
12 **supplementary material (section 3).**The extra saturator tests, mentioned in section 3.1 and found  
13 in supplementary material, showed that the carrier gas used in this experiment was at least as  
14 pure as the most pure gas available commercially (AGA, N<sub>2</sub>, 6.0), which has impurities less  
15 than 1 ppm, including hydrocarbons less than 0.1 ppm. According to the results found in  
16 supplementary material, the actions taken to purify the carrier gas in these experiments were  
17 sufficient. Nevertheless, there were contaminants left in the carrier gas at levels which will  
18 affect the nucleation process.

#### 20 **4 Discussion and Conclusions**

21 A saturator was used to produce sulphuric-acid vapour from neat-liquid sulphuric acid for  
22 laboratory studies. It was tested and shown to produce similar apparent formation rates at  
23 similar conditions to our previous vapour-production method of the furnace. The sulphuric-acid  
24 or total-sulphate concentration was measured with two independent methods and it was shown  
25 to produce exact concentrations as prediction from Richardson et al. (1986) and slightly higher  
26 than the prediction from Kulmala and Laaksonen (1990) when measured with MARGA (Fig.  
27 3). Concentrations of sulphuric-acid monomer measured with CIMS and CI-Api-TOF was one-  
28 to-two orders-of-magnitude lower than the total-sulphate values measured with MARGA and  
29 the prediction by Eq. (1) and (2). The only source of sulphuric acid (sulphate measured by  
30 MARGA) is the liquid sulphuric acid inside the saturator as seen in Fig. 3. A possible reason  
31 for the discrepancy is that the sulphuric acid is in particle phase since the saturator is a  
32 substantial source of particles. However, these particles are lost on the way from the saturator

1 to the nucleation chamber due to two main reasons: (i) the flowrate (0.5 lpm) in the tube (length:  
2 1 m, I.D. 4 mm) from the saturator to the nucleation chamber is relatively low increasing  
3 diffusional losses and (ii) the highly turbulent mixing of the saturator flow with the mixing flow  
4 ( $Q_{sat} : Q_{mix} \approx 1:30$  or more) transforms the mixer into an effective trap for the particles. The loss  
5 of the particles is confirmed with DMPS measurements which cannot explain the discrepancy  
6 (supplementary material, Fig. S1). Maximum losses to the particle phase in the flow tube are 0-  
7 1.4 % with an average below 1 % of the total sulphate. The discrepancy cannot be explained by  
8 the formation of larger clusters containing solely sulphuric acid (dimer, trimer, etc.) either,  
9 because the concentration of these clusters is in the order of few percent or lower than the  
10 monomer concentration (Supplementary material, Fig. S5).

11 The characteristics of the freshly nucleated particles together with the conditions used for the  
12 nucleation has been identified and presented (Fig. 4-7). Total losses of sulphuric acid or total  
13 sulphate to the whole flow-tube setup have been determined for both methods to detect the  
14 concentration of sulphuric acid or total sulphate.

15 The average Total Loss Factors determined are  $TLF = 10.0 \pm 1.2$  ( $T_{sat} = 284-297$  K) for  
16 MARGA and  $TLF = 14.2 \pm 4.2$  ( $T_{sat} = 286-300$  K) for CIMS both having a slight increasing  
17 deviation from the first-order losses as a function of saturator temperature (Fig. 4). The second-  
18 order losses are caused by losses to the particles and losses to the clusters which are too small  
19 to be detected by particle counters.

20 Formation rates of sulphuric acid-water system were compared to our previous studies (Brus et  
21 al., 2010 and 2011), where a method of the furnace was used (Fig. 8-10). Obtained apparent  
22 formation rates as a function of sulphuric-acid or total-sulphate concentrations were  
23 independent of the sulphuric-acid vapour-production method (furnace vs saturator). Conditions  
24 for these studies were similar ( $T = 298$  K, RH ~30 %) but at similar formation rates, the  
25 sulphuric-acid monomer concentration is one-to-two orders-of-magnitude lower than the total  
26 sulphate. The slope of the fit to the formation-rate data as a function of sulphuric-acid monomer  
27 concentration ( $1.3 \pm 0.2$ ) is very similar as obtained in Brus et al. (2011) ( $1.2 \pm 0.1$ ). The  
28 comparison to our previous measurements was done to check reproducibility of the nucleation-  
29 experiment results between the sulphuric-acid vapour-production methods and to eliminate the  
30 production method as a possible reason for the discrepancy. The discussion and interpretation  
31 of the slopes (section 3.1) and comparison to the atmospheric data (section 3.5) can be found  
32 in Brus et al. (2011).

1 Other possible reasons for this difference between sulphuric acid monomer and total sulphate  
2 is that sulphuric acid molecules are most probably bond to some molecule(s) (e.g. amines,  
3 ammonia, organics) and not been detected by CIMS or identified from the CI-API-TOF spectra  
4 (Kulmala et al., 2013). As Kurten et al., (2011) state, base molecules can be only in minor  
5 importance due to the fact that nitrate ion ( $\text{NO}_3^-$ ) will most probably substitute the base out in  
6 the CIMS charging process. Nevertheless, there is expected to be a substantial pool of clusters  
7 formed of sulphuric acid-base molecules in our system, which are too small to be detected by  
8 current state-of-art particle counters such as PSM. These clusters are the main reason for the  
9 discrepancy between measured total sulphate and the monomer concentrations. Same or similar  
10 clusters are most probably forming in all laboratory nucleation experiments involving sulphuric  
11 acid, as there are always contaminants present in the carrier gases (see supplementary material,  
12 section 6 and Figs. S6 to S11). Average ammonia concentration of 60 pptv was found in the  
13 system for dry conditions and 126 pptv for RH 30 % as a contaminant and it was independent  
14 of the saturator temperature. It is assumed to originate from the purified, dry, particle-free air  
15 used as carrier gas and from the ultrapure water used for humidifying the mixing flow.  
16 Ammonia concentration is enough to affect the nucleation process itself substantially but the  
17 magnitude of this effect was not studied in this work. Ammonia can bind sulphuric acid by  
18 forming clusters, which might reduce the monomer concentration measured with CIMS and CI-  
19 Api-TOF slightly. Since the contaminant level was constant and saturator temperature was  
20 increased, reducing the contaminant to total sulphate-ratio from ~1:1 to ~1:10 for dry conditions  
21 and from ~3:1 to ~1:5 for humid conditions, does not explain the discrepancy between the two  
22 sulphuric-acid- or total-sulphate-detection methods. Even though the contaminant levels might  
23 sound high, those are still below the most-pure commercially available gases (AGA,  $\text{N}_2$ , 6.0).

24 Other possible reasons for the difference between sulphuric acid monomer and total sulphate is  
25 that sulphuric acid molecules are most probably bonded to some molecule(s) (e.g. amines,  
26 ammonia, organics) and not detected by CIMS or identified from the CI-API-TOF spectra  
27 (Kulmala et al., 2013). As Kurten et al. (2011) state, base molecules can be only in minor  
28 importance due to the fact that nitrate ion ( $\text{NO}_3^-$ ) will most probably substitute the base out in  
29 the CIMS charging process. Nevertheless, there is expected to be a substantial pool of clusters  
30 formed of sulphuric acid-base molecules in our system, which are too small to be detected by  
31 current state-of-art particle counters such as PSM. These clusters are the main reason for the  
32 discrepancy between measured total-sulphate and the monomer concentrations. Same or similar  
33 clusters are most probably forming in all laboratory nucleation experiments involving sulphuric

1 acid, as there are always contaminants present in carrier gases. Further analysis of the CI-Api-  
2 TOF mass spectra showed a large number of stick-unit masses correlating with sulphuric-acid  
3 monomer ion ( $\text{HSO}_4^-$ ) suggesting a large number of clusters containing sulphuric acid which  
4 are not used for calculating the sulphuric-acid concentration measured by mass spectrometers  
5 (see supplementary material, section 6 and Fig. S6-S11). Sulphuric acid (measured here as  
6 sulphate) can contribute to the early growth of ultrafine particles to a much larger extent than  
7 currently thought, since most of the sulphuric acid remains undetected. Also the huge number  
8 of correlating masses with increasing sulphuric-acid concentration implies that there are  
9 numerous substances that can form stable clusters with sulphuric acid that may be the starting  
10 point for particle formation.

11 The total sulphate (originally total sulphuric acid) is responsible for the particle growth as  
12 demonstrated in Skrabalova et al. (2014). The contribution of the total sulphate to the nucleation  
13 process itself is not yet fully understood. However, recent results suggest that sulphuric acid  
14 monomer is the main component in nucleation (Brus et al., 2014) and not the overall sulphuric  
15 acid. To find out which molecules are possibly involved in nucleation, the clusters with  
16 sulphuric acid must be identified from the CI-Api-TOF spectra.

## 17

### 18 **Acknowledgements**

19 The financial support by the Academy of Finland Centre of Excellence program (project no.  
20 1118615), KONE foundation and by the Maj and Tor Nessling Foundation are gratefully  
21 acknowledged. The language improvements provided by Curtis Wood are gratefully  
22 acknowledged.

1  
2  
3  
4  
5  
6  
7  
8  
9  
10  
11  
12  
13  
14  
15  
16  
17  
18  
19  
20  
21  
22  
23  
24  
25

**References**

Arnold., F.: Ion-induced nucleation of atmospheric water vapor at the mesopause, *Planetary and Space Science*, 28, 10, 1003-1009, doi: 10.1016/0032-0633(80)90061-6, 1980.

Ayers, G. P., Gillett, R. W. and Gras, J. L.: On the vapor pressure of sulphuric acid, *Geophys. Res. Letters*, 7, 6, 433-436, 1980.

Ball, S. M., Hanson, D. R. and Eisele, F. L.: Laboratory studies of particle nucleation: Initial results for H<sub>2</sub>SO<sub>4</sub>, H<sub>2</sub>O, and NH<sub>3</sub> vapors, *J. of Geophys. Res.*, 104, D19, 23,709-23,718, doi: 10.1029/1999JD900411, 1999.

Benson, D., Young, L.-H., Kameel, F. and Lee, S.-H.: Laboratory-measured nucleation rates of sulfuric acid and water binary homogeneous nucleation from the SO<sub>2</sub> + OH reaction, *Geophys. Res. Lett.*, 35, L11801, doi:10.1029/2008GL033387, 2008.

1 Benson, D. R., Erupe, M. E. and Lee, S.-H.: Laboratory-measured H<sub>2</sub>SO<sub>4</sub>-H<sub>2</sub>O-NH<sub>3</sub> ternary  
2 homogeneous nucleation rates: Initial observations, *Geophys. Res. Letters*, 36, L15818,  
3 doi:10.1029/2009GL038728, 2009.

4 Benson, D. R., Yu, J. H., Markovich, A. and Lee, S.-H.: Ternary homogeneous nucleation of  
5 H<sub>2</sub>SO<sub>4</sub>, NH<sub>3</sub>, and H<sub>2</sub>O under conditions relevant to the lower troposphere, *Atmos. Chem. Phys.*,  
6 11, 4755-4766, doi: 10.5194/acp-11-4755-2011, 2011.

7 Berndt, T., Stratmann, F., Bräsel, S., Heintzenberg, J., Laaksonen, A. and Kulmala, M.: SO<sub>2</sub>  
8 oxidation products other than H<sub>2</sub>SO<sub>4</sub> as a trigger of new particle formation. Part 1: Laboratory  
9 investigations, *Atmos. Chem. Phys.*, 8, 6365-6374, 2008.

10 Berndt, T., Stratmann, F., Sipilä, M., Vanhanen, J., Petäjä, T., Mikkilä, J., Gruner, A., Spindler,  
11 G., Lee Mauldin III, R., Curtius, J., Kulmala, M. and Heintzenberg, J.: Laboratory study on  
12 new particle formation from the reaction OH + SO<sub>2</sub>: influence of experimental conditions, H<sub>2</sub>O  
13 vapour, NH<sub>3</sub> and the amine tert-butylamine on the overall process, *Atmos. Chem. Phys.*, 10,  
14 7101-7116, doi:10.5194/acp-10-7101-2010, 2010.

15 Berresheim, H., Elste, T., Plass-Dülmer, C. Eisele, F. L. and Tanner, D. J.: Chemical ionization  
16 mass spectrometer for long-term measurements of atmospheric OH and H<sub>2</sub>SO<sub>4</sub>, *Int. J. of Mass*  
17 *Spectr.* 202, 91-109, 2000.

18 Brus, D., Hyvärinen, A.-P., Viisanen, Y., Kulmala, M. and Lihavainen H.: Homogeneous  
19 nucleation of sulfuric acid and water mixture: experimental setup and first results, *Atmos.*  
20 *Chem. Phys.*, 10, 2631-2641, 2010.

21 Brus, D., Neitola, K., Petäjä, T., Vanhanen, J., Hyvärinen, A.-P., Sipilä, M., Paasonen, P.,  
22 Lihavainen H. and Kulmala, M.: Homogenous nucleation of sulfuric acid and water at  
23 atmospherically relevant conditions, *Atmos. Chem. Phys.*, 11, 5277-5287, doi:10.5194/acp-11-  
24 5277-2011, 2011.

25 Brus, D., Hyvärinen, A.-P., Anttila, T., Neitola, K., Koskinen, J., Makkonen, U., Hellén, H.,  
26 Hemmilä, M., Sipilä, M., Mauldin III, R. L., Jokinen, T., Petäjä, T., Kurtén, T., Vehkamäki, H.,  
27 Kulmala, M., Viisanen, Y., Lihavainen, H., and Laaksonen, A.: Reconsidering the sulphuric  
28 acid saturation vapour pressure: Classical Nucleation Theory revived, *Physical Review Letters*,  
29 in review, (2014).

30 Davidson, C., Phalen, R. and Solomon P.: Airborne Particulate Matter and Human Health: a  
31 Review, *Aerosol Sci. and Tech.*, 39, 8, 2005.

1 Eisele, F. and Tanner, D.: Measurement of the gas phase concentration of H<sub>2</sub>SO<sub>4</sub> and methane  
2 sulfonic acid and estimates of H<sub>2</sub>SO<sub>4</sub> production and loss in the atmosphere, *J. Geophys. Res.*,  
3 98, D5, 9001-9010, doi:10.1029/93JD00031, 1993.

4 Feingold G. and Siebert, H.: Chapter 14 Cloud-Aerosol Interactions from the Micro to the  
5 Cloud Scale, in *Clouds in the Perturbed Climate System*, edited by J. Heintzenberg and R.J.  
6 Charlson, pp. p. 576, The MIT Press, Cambridge, 2009.

7 Herrmann, E., Brus, D., Hyvärinen, A.-P., Stratmann, F., Wilck, M., Lihavainen, H. and  
8 Kulmala, M.: A computational fluid dynamics approach to nucleation in the water-sulfuric acid  
9 system, *J. Phys. Chem. A*, 114 (31), 8033-8042, 2010.

10 Hirsikko, A., Nieminen, T., Gagné, S., Lehtipalo, K., Manninen, H. E., Ehn, M., Hörrak, U.,  
11 Kerminen, V.-M., Laakso, L., McMurry, P. H., Mirme, A., Mirme, S., Petäjä, T., Tammet, H.,  
12 Vakkari, V., Vana, M. and Kulmala, M.: Atmospheric ions and nucleation: a review of  
13 observations, *Atmos. Chem. Phys.*, 11, 767-798, doi:10.5194/acp-11-767-2011, 2011.

14 Jokinen, V. and Mäkelä, J. M.: Closed-loop arrangement with critical orifice for DMA sheath/  
15 excess flow system. *J. Aerosol Sci.*, 28, 643-648, 1997.

16 Jokinen, T., Sipilä, M., Junninen, H., Ehn, M., Lönn, G., Hakala, J., Petäjä, T., Mauldin III, R.  
17 L., Kulmala, M., and D. R. Worsnop, D. R.: Atmospheric sulphuric acid and neutral cluster  
18 measurements using CI-API-TOF. *Atmos. Chem. Phys.*, 12, 4117-4125, doi:10.5194/acp-12-  
19 4117-2012, 2012.

20 Junninen, H., Ehn, M., Petäjä, T., Luosujärvi, L., Kotiaho, T., R. Kostianen, R., Rohner, U.,  
21 Gonin, M., Fuhrer, K., Kulmala, M. and Worsnop, D.: A high-resolution mass spectrometer to  
22 measure atmospheric ion composition, *Atmos. Meas. Tech.*, 3, 1039-1053, doi:10.5194/amt-3-  
23 1039-2010, 2010.

24 Kerminen, V.-M. Petäjä, T., Manninen, H. E., Paasonen, P., Nieminen, T., Sipilä, M., Junninen,  
25 H., Ehn, M., Gagné, S., Laakso, L., Riipinen, I., Vehkamäki, H., Kurten, T., Ortega, I. K., Dal  
26 Maso, M., Brus, D., Hyvärinen, A.-P., Lihavainen, H., Leppä, J., Lehtinen, K. E. J., Mirme, A.,  
27 Mirme, S., Horrák, U., Berndt, T., Stratmann, F., Birmili, W., Wiedensohler, A., Metzger, A.,  
28 Dommen, J., Baltensperger, U., Kiendler-Scharr, A., Mentel, T. F., Wildt, J., Winkler, P. M.,  
29 Wagner, P. E., Petzold, A., Minikin, A., Plass-Dülmer, C., Pöschl, U., Laaksonen, A. and M.  
30 Kulmala, M.: Atmospheric nucleation: highlights of the EUCAARI project and future  
31 directions, *Atmos. Chem. Phys.*, 10, 10829-10848, doi:10.5194/acp-10-10829-2010, 2010.



1 Kirkby, J., Curtius, J., Almeida, J., Dunne, E., Duplissy, J., Ehrhart, S., Franchin, A., Gagné,  
2 S., Ickes, L., Kürten, A., Kupc, A., Metzger, A., Riccobono, F., Rondo, L., Schobesberger,  
3 S., Tsagkogeorgas, G., Wimmer, D., Amorim, A., Bianchi, F., Breitenlechner, M., David, A.,  
4 Dommen, J., Downard, A., Ehn, M., Flagan, R., Haider, S., Hansel, A., Hauser, D., Jud, W.,  
5 Junninen, H., Kreissl, F., Kvashin, A., Laaksonen, A., Lehtipalo, K., Lima, J., Lovejoy, E.,  
6 Makhmutov, V., Mathot, S., Mikkilä, J., Minginette, P., Mogo, S., Nieminen, T., Onnela, A.,  
7 Pereira, P., Petäjä, T., Schnitzhofer, R., Seinfeld, J., Sipilä, M., Stozhkov, Y., Stratmann, F.,  
8 Tomé, A., Vanhanen, J., Viisanen, Y., Aron Vrtala, A., Wagner, P., Walther, H., Weingartner,  
9 E., Wex, H., Winkler, P., Carslaw, K., Worsnop, D., Baltensperger, U. and Kulmala, M.: Role  
10 of sulphuric acid, ammonia and galactic cosmic rays in atmospheric aerosol nucleation, *Nature*,  
11 476, 429-433, doi:10.1038/nature10343, 2011.

12 Korhonen, P., Kulmala, M., Laaksonen, A., Viisanen, Y., McGraw, R., and Seinfeld, J. H.:  
13 Ternary nucleation of H<sub>2</sub>SO<sub>4</sub>, NH<sub>3</sub> and H<sub>2</sub>O in the atmosphere, *J. Geophys. Res.*, 104, 26 349-  
14 26 353, doi: 10.1029/1999JD900784, 1999.

15 Kulmala M. and Laaksonen, A.: Binary nucleation of water-sulfuric acid system: Comparison  
16 of classical theories with different H<sub>2</sub>SO<sub>4</sub> saturation vapor pressures, *J. Chem. Phys.*, 93 (1). 1,  
17 doi: 10.1063/1.459519, 1990.

18 Kulmala, M., Vehkamäki H., Petäjä T., Dal Maso M., Lauri A., Kerminen V.-M., Birmili W.  
19 and McMurry P. H.: Formation and growth rates of ultrafine atmospheric particles: A review  
20 of observations, *J. Aerosol Sci.*, 35, 143-176, doi: 10.1016/j.jaerosci.2003.10.003, 2004a.

21 Kulmala, M., Lehtinen, K. E. J., and Laaksonen, A.: Cluster activation theory as an explanation  
22 of the linear dependence between formation rate of 3 nm particles and sulphuric acid  
23 concentration, *Atmos. Chem. Phys.*, 6, 787-793, 2006.

24 Kulmala, M., Riipinen, I., Sipilä, M., Manninen, H. E., Petäjä, T., Junninen, H., Dal Maso, M.,  
25 Mordas, G., Mirme, A., Vana, M., Hirsikko, A., Laakso, L., Harrison, R. M., Hanson, I., Leung,  
26 C., Lehtinen, K. E. J., Kerminen, V.-M.: Towards direct measurement of atmospheric  
27 nucleation, *Science*, 318, 89, DOI: 10.1126/science.1144124, 2007.

28 Kulmala, M., Petäjä, T., Nieminen, T., Sipilä, M., Manninen, H. E., Lehtipalo, K., Dal Maso,  
29 M., Aalto, P. P., Junninen, H., Paasonen, P., Riipinen, I., Lehtinen K. E. J., Laaksonen Kari E  
30 J and Kerminen, V.-M.: Measurement of the nucleation of atmospheric aerosol particles, *Nature*  
31 *protocols*, 7, 9, doi:10.1038/nprot.2012.091, 2012.

1 Kulmala, M., Kontkanen, J., Junninen, H., Lehtipalo, K., Manninen, H. E., Nieminen, T.,  
2 Petäjä, T., Sipilä, M., Schobesberger, S., Rantala, P., Franchin, A., Jokinen, T., Järvinen, E.,  
3 Äijälä, M., Kangasluoma, J., Hakala, J., Aalto, P. P., Paasonen, P., Mikkilä, J., Vanhanen, J.,  
4 Aalto, J., Hakola, H., Makkonen, U., Ruuskanen, T., Mauldin III, R. L., Duplissy, J.,  
5 Vehkamäki, H., Bäck, J., Kortelainen, A., Riipinen, I., Kurten, T., Johnston, M. V., Smith, J.  
6 N., Ehn, M., Mentel, T. F., Lehtinen, K. E. J., Laaksonen, A., Kerminen, V.-M. and Worsnop,  
7 D. R.: Direct observations of atmospheric aerosol nucleation, *Science*, 339, 6122, 943-946,  
8 2013.

9 Kürten, A., Rondo, L., Ehrhart, S. and Curtius, J.: Calibration of a Chemical Ionization Mass  
10 Spectrometer for the Measurement of Gaseous Sulfuric Acid, *J. Phys. Chem. A*, 116, 6375-  
11 6386, 2012.

12 Lee, S.-H., Reeves, J. M., Wilson, J. C., Hunton, D. E., Viggiano, A. A., Miller, T. M.,  
13 Ballenthin, J. O., Lait, L. R.: Particle Formation by Ion Nucleation in the Upper Troposphere  
14 and Lower Stratosphere, *Science*, 301, 5641, 1886-1889, doi: 10.1126/science.1087236, 2003.

15 Lovejoy, E. R., Curtius, J., and Froyd, K. D.: Atmospheric ion-induced nucleation of sulphuric  
16 acid and water, *J. Geophys. Res.*, 109, D08204, doi:10.1029/2003JD004460, 2004.

17 Lihavainen, H., Kerminen, V.-M., Komppula, M., Hatakka, J., Aaltonen, V., Kulmala, M. and  
18 Viisanen Y.: Production of “potential” cloud condensation nuclei associated with atmospheric  
19 new-particle formation in northern Finland, *J. Geophys. Res.*, 108(D24), 4782,  
20 doi:10.1029/2003JD003887, 2003.

21 Makkonen, U., Virkkula, A., Mäntykenttä, J., Hakola, H., Keronen, P., Vakkari, V. and Aalto,  
22 P. P.: Semi-continuous gas and inorganic aerosol measurements at a Finnish urban site:  
23 comparisons with filters, nitrogen in aerosol and gas phases, and aerosol acidity, *Atmos. Chem.*  
24 *Phys.*, 12, 5617-5631, doi:10.5194/acp-12-5617-2012, 2012.

25 Manninen, H. E., Nieminen, T., Asmi, E., Gagné, S., Häkkinen, S., Lehtipalo, K., Aalto, P.,  
26 Vana, M., Mirme, A., Mirme, S., Hörrak, U., Plass-Dülmer, C., Stange, G., Kiss, G., Hoffer,  
27 A., Törö, N., Moerman, M., Henzing, B., de Leeuw, G., Brinkenberg, M., Kouvarakis, G. N.,  
28 Bougiatioti, A., Mihalopoulos, N., O’Dowd, C., Ceburnis, D., Arneth, A., Svenningsson, B.,  
29 Swietlicki, E., Tarozzi, L., Decesari, S., Facchini, M. C., Birmili, W., Sonntag, A.,  
30 Wiedensohler, A., Boulon, J., Sellegri, K., P. Laj, P., Gysel M., Bukowiecki, N., Weingartner,  
31 E., Wehrle, G., Laaksonen, A., Hamed, A., J. Joutsensaari, J., Petäjä, T., Kerminen, V.-M. and

1 Kulmala, M.: EUCAARI ion spectrometer measurements at 12 European sites - analysis of new  
2 particle formation events, *Atmos. Chem. Phys.*, 10, 7907-7927, doi: 10.5194/acp-10-7907-  
3 2010, 2010.

4 Mauldin III, R. L., Frost, G., Chen, G., Tanner, D., Prevot, A., Davis, D., and Eisele, F.: OH  
5 measurements during the First Aerosol Characterization Experiment (ACE 1): Observations  
6 and model comparisons, *J. Geophys. Res.*, 103, 16713-16729, doi:10.1029/98JD00882, 1998.

7 Merikanto, J., Spracklen, D. V., Mann, G. W., Pickering, S. J., and Carslaw, K. S.: Impact of  
8 nucleation on global CCN, *Atmos. Chem. Phys.*, 9, 8601-8616, 2009.

9 Napari, I., Noppel, M., Vehkamäki, H. and Kulmala M.: Parametrization of ternary nucleation  
10 rates for  $\text{H}_2\text{SO}_4\text{-NH}_3\text{-H}_2\text{O}$  vapors, *J. Geophys. Res.*, 107(D19), 4381,  
11 doi:10.1029/2002JD002132, 2002.

12 Nieminen, T., Paasonen, P., Manninen, H. E., Sellegri, K., Kerminen, V.-M. and Kulmala, M.:  
13 Parameterization of ion-induced nucleation rates based on ambient observations, *Atmos. Chem.*  
14 *Phys.*, 11, 3393-3402, doi:10.5194/acp-11-3393-2011, 2011.

15 Paasonen, P., Nieminen, T., Asmi, E., Manninen, H. E., Petäjä, T., Plass-Dülmer, C., Flentje,  
16 H., Birmili, W., Wiedensohler, A., Horrák, U., Metzger, A., Hamed, A., Laaksonen, A.,  
17 Facchini, M. C., Kerminen, V.-M. and Kulmala, M.: On the roles of sulphuric acid and low-  
18 volatility organic vapours in the initial steps of atmospheric new particle formation, *Atmos.*  
19 *Chem. Phys.*, 10, 11223-11242, doi:10.5194/acp-10-11223-2010, 2010.

20 Petäjä, T., Mauldin, III, R., Kosciuch, E., McGrath, J., Nieminen, T., Paasonen, P., Boy, M.,  
21 Adamov, A., Kotiaho, T. and Kulmala M.: Sulfuric acid and OH concentrations in a boreal  
22 forest site, *Atmos. Chem. Phys.*, 9, 7435-7448, 2009.

23 Richardson, C. B., Hightower, R. L. and Pigg, A. L.: Optical measurements of evaporation of  
24 sulphuric acid droplets, *Applied Optics*, 25, 7, 1226-1229, 1986.

25 Sipilä, M., Berndt, T., Petäjä, T., Brus, D., Vanhanen, J., Stratmann, F., Patokoski, J., Mauldin  
26 III, Roy L., Hyvärinen, A.-P., Lihavainen, H. and Kulmala, M.: The role of sulphuric acid in  
27 atmospheric nucleation, *Science*, 327, 5970, 1243-1246, doi: 10.1126/science.1180315, 2010.

28 Škrabalová L., Brus, D., Anttila, T., Ždímal, V. and Lihavainen H.: Growth of sulphuric acid  
29 nanoparticles under wet and dry conditions, *Atmos. Chem. Phys.* 14, 6461-6475,  
30 doi:10.5194/acp-14-6461-2014, 2014.

1 Slanina, J., ten Brink, H. M., Otjes, R. P., Even, A., Jongejan, P., Khlystov, S., Waijers-Ijpelaan,  
2 A., Hu, M., and Lu, Y.: The continuous analysis of nitrate and ammonium in aerosols by the  
3 steam jet aerosol collector (SJAC): extension and validation of the methodology, *Atmos.*  
4 *Environ.*, 35, 2319-2330, doi:10.1016/S1352-2310(00)00556-2, 2001.

5 Spracklen, D. V., Carslaw, K. S., Kulmala, M., Kerminen, V.-M., Mann, G. W. and Sihto, S.  
6 L.: The contribution of boundary layer nucleation events to total particle concentration on  
7 regional and global scales, *Atmos. Chem. Phys.*, 6, 5631-5648, 2006.

8 ten Brink, H., Otjes, R., Jongejan, P. and Slanina S.: An instrument for semi-continuous  
9 monitoring of the size-distribution of nitrate, ammonium, sulphate and chloride in aerosol,  
10 *Atmos. Environ.*, 41, 13, 2768-2779, 10.1016/j.atmosenv.2006.11.041, 2007.

11 Vanhanen, J., Mikkilä, J., Lehtipalo, K., M. Sipilä, M., Manninen, H., Siivola, E., Petäjä, T.  
12 and Kulmala, M.: *Aerosol Sci. and Tech.*, 45, 4, 533-542, doi:10.1080/02786826.2010.547889,  
13 2011.

14 Vehkamäki, H., Kulmala, M., Napari, I., Lehtinen, K. E. J., Timmreck, C., Noppel, M. and  
15 Laaksonen A.: An improved parameterization for sulfuric acid-water nucleation rates for  
16 tropospheric and stratospheric conditions, *J. Geophys. Res.*, 107(D22), 4622,  
17 doi:10.1029/2002JD002184, 2002.

18 Viisanen, Y., Kulmala, M. and Laaksonen, A.: Experiments on gas-liquid nucleation of sulfuric  
19 acid and water, *J. Chem. Phys.* 107, 920; doi: 10.1063/1.474445, 1997.

20 Weber, R. J., Marti, J. J., McMurry, P. H., Eisele, F. L., Tanner, D. J. and Jefferson, A.:  
21 Measured atmospheric new particle formation rates: Implications for nucleation mechanisms,  
22 *Chemical Engineering Communications*, 151, 53-64, doi: 10.1080/00986449608936541, 1996.

23 Wiedensohler, A. and Fissan, H. J.: Bipolar Charge Distributions of Aerosol Particles in High-  
24 Purity Argon and Nitrogen, *Aerosol Sci. and Tech.*, 14:358-364, doi:  
25 10.1080/02786829108959498, 1991.

26 Winkler, P. M., Steiner, G., Vrtala, A., Vehkamäki, H., Noppel, M., Lehtinen, K. E. J., Reischl,  
27 G. P., Wagner, P. E., Kulmala, M.: Heterogeneous Nucleation Experiments Bridging the Scale  
28 from Molecular Ion Clusters to Nanoparticles, *Science*, 319, 5868,1374-1377, doi:  
29 10.1126/science.1149034, 2008.

1 Wyslouzil, B. E., Seinfeld, J. H. and Flagan, R. C.: Binary nucleation in acid-water systems. I.  
2 Methanesulfonic acid-water, *J. Chem. Phys.* 94, 6842, 1991.

3 Young, L., Benson, D., Kameel, F., Pierce, J., Junninen, H., Kulmala, M. and Lee, S.-H.:  
4 Laboratory studies of H<sub>2</sub>SO<sub>4</sub>/H<sub>2</sub>O binary homogeneous nucleation from the SO<sub>2</sub>+OH reaction:  
5 evaluation of the experimental setup and preliminary results, *Atmos. Chem. Phys.*, 8, 4997-  
6 5016, 2008.

7 Yu, F.: From molecular clusters to nanoparticles: second-generation ion-mediated nucleation  
8 model, *Atmos. Chem. Phys.*, 6, 5193-5211, 2006.

9 Yu, F., Wang, Z., Luo, G. and Turco R.: Ion-mediated nucleation as an important global source  
10 of tropospheric aerosols, *Atmos. Chem. Phys.*, 8, 2537-2554, 2008.

11 Yu, F.: Ion-mediated nucleation in the atmosphere: Key controlling parameters, implications,  
12 and look-up table, *J. of Geophys. Res.*, 115, D03206, doi:10.1029/2009JD012630, 2010.

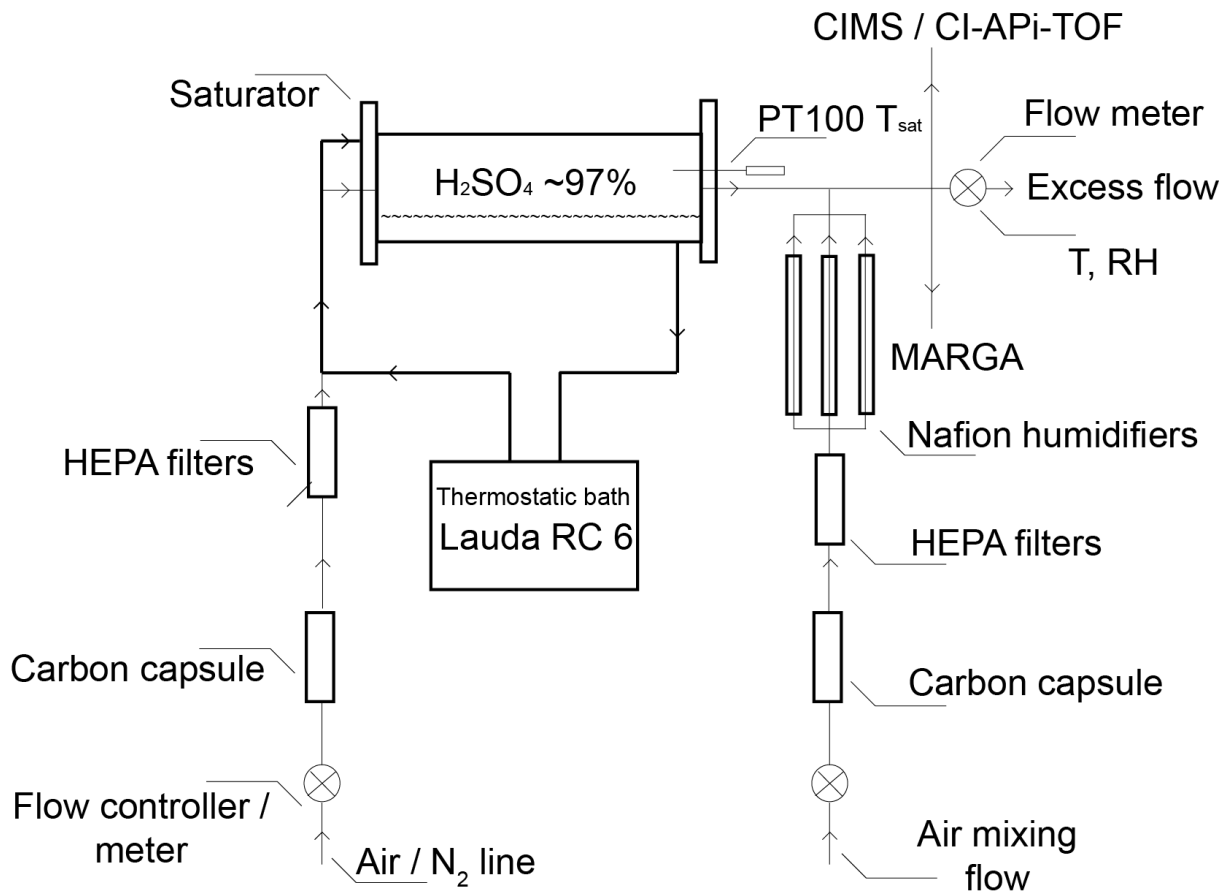
13 Zhang, R., Khalizov, A. F., Wang, L., Hu, M., Xu, W.: Nucleation and growth of nanoparticles  
14 in the atmosphere, *Chem. Rev.* 112, 1957-2011, doi: 10.1021/cr2001756 2012.

15 Zheng, J., Khalizov, A., Wang, L. and Zhang, R.: Atmospheric Pressure-Ion Drift Chemical  
16 Ionization Mass Spectrometry for Detection of Trace Gas Species, *Anal. Chem.*, 82, 7302-7308,  
17 doi: 10.1021/ac101253n, 2010.

18 Zollner, J. H., Glasoe, W. A., Panta, B., Carlson, K. K., McMurry, P. H. and Hanson, D. R.:  
19 Sulfuric acid nucleation: power dependencies, variation with relative humidity, and effect of  
20 bases, *Atmos. Chem. Phys.*, 12, 4399-4411, doi:10.5194/acp-12-4399-2012, 2012.

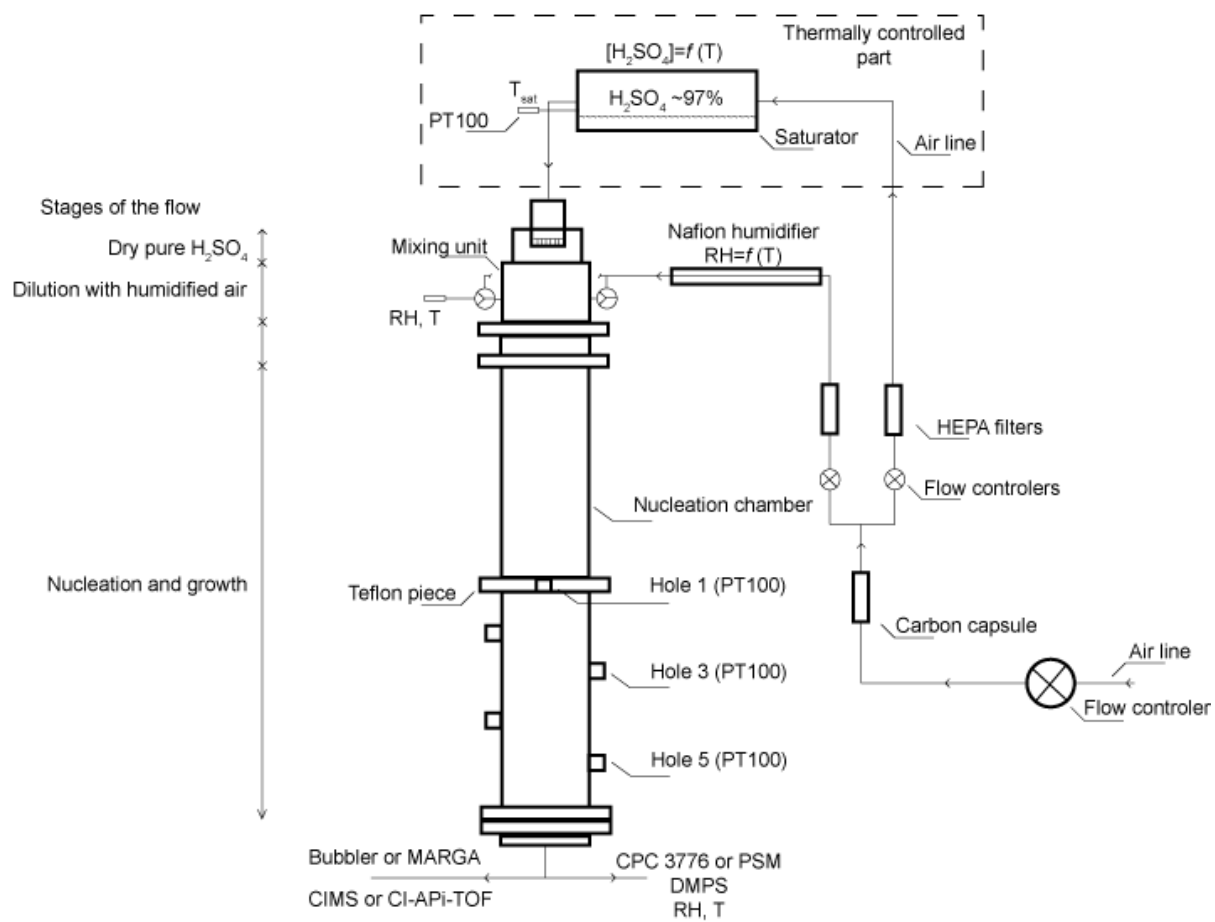
21  
22  
23  
24  
25  
26  
27  
28

1  
2  
3



4  
5  
6

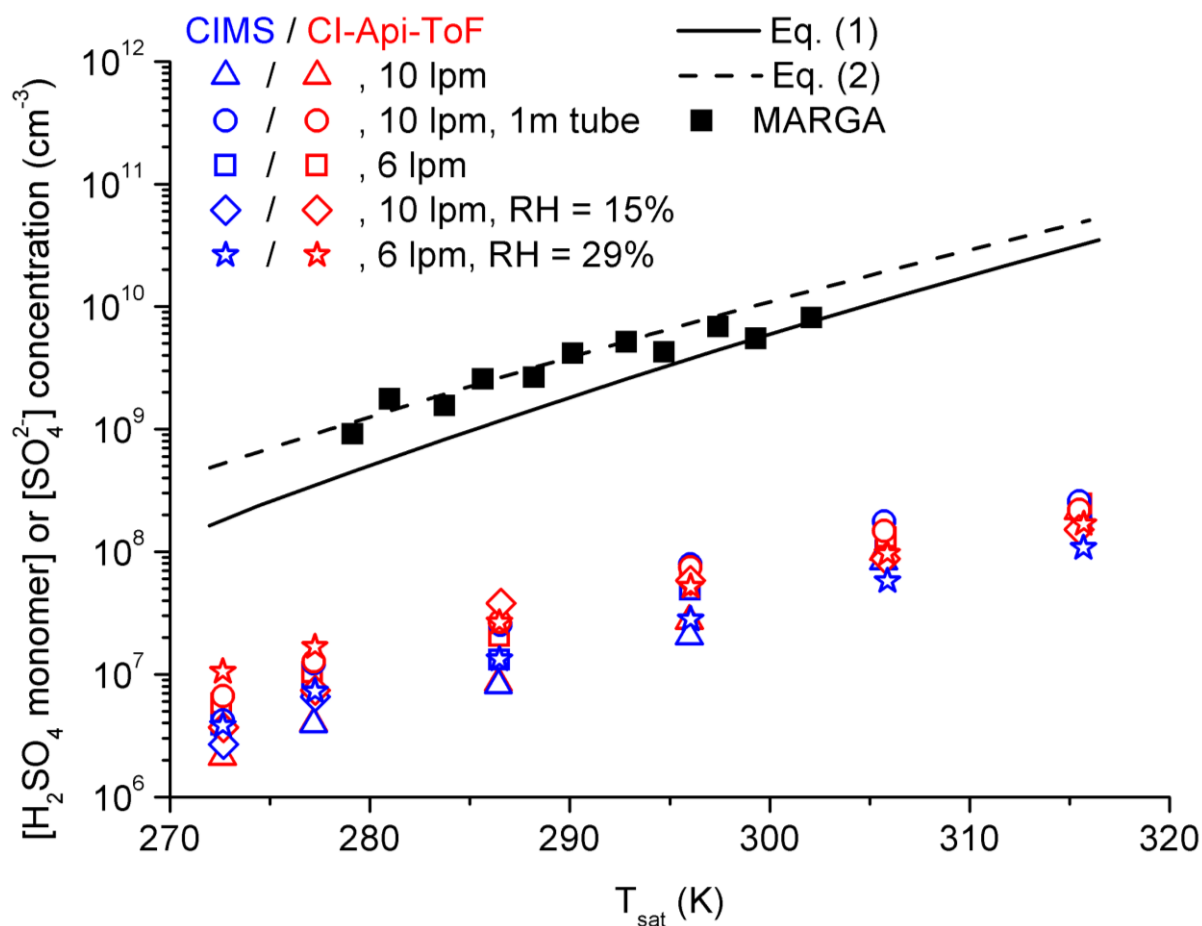
Figure 1. Schematic figure of the setup for testing the saturator.



1

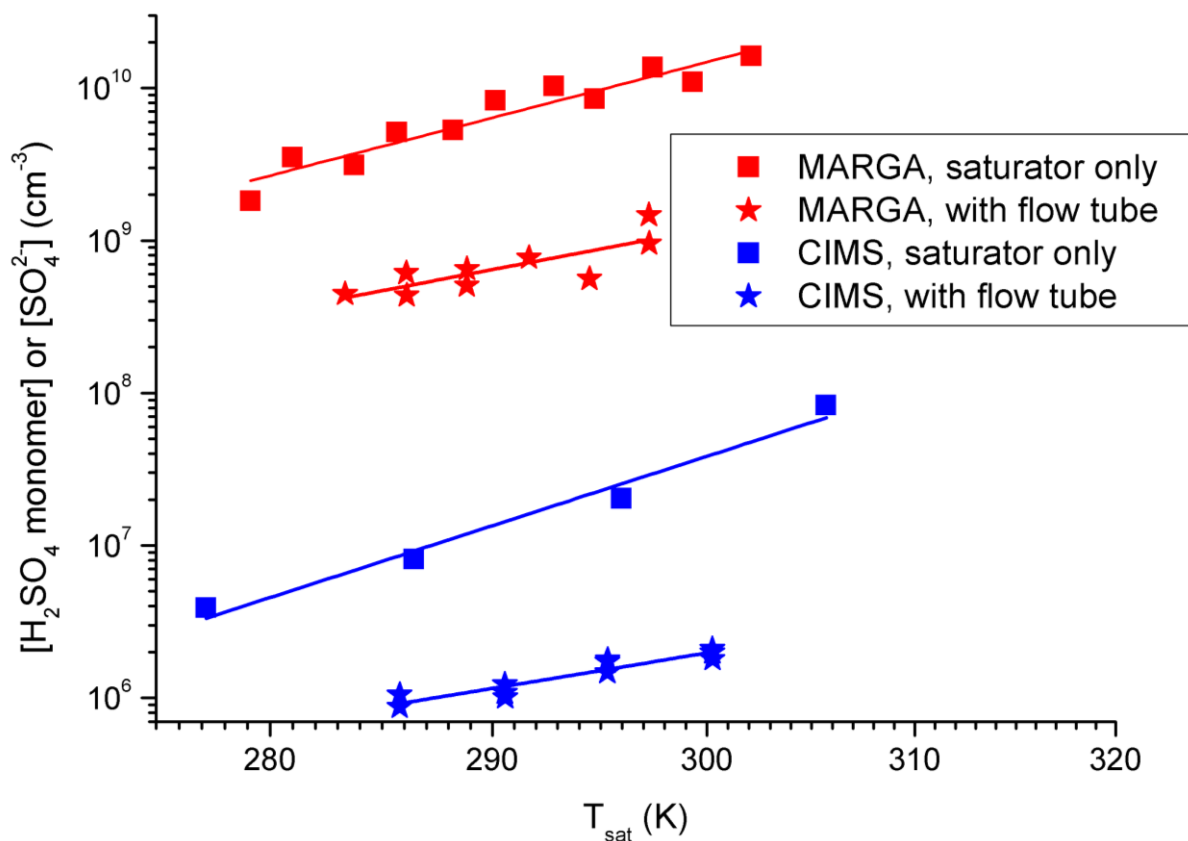
2

3 Figure 2. Flow-tube setup.



1  
 2  
 3 Figure 3. Measured sulphuric-acid monomer  $[H_2SO_4 \text{ monomer}]$  and total-sulphate  $[SO_4^{2-}]$   
 4 (black squares) concentrations together with predicted values by Eq. (1) and (2) as a function  
 5 of saturator temperature  $T_{\text{sat}}$ . Saturator flowrate is  $Q_{\text{sat}} = 0.5 \text{ lpm}$  and mixing flowrates were 40  
 6 lpm (dry for CIMS and CI-Api-TOF and RH 15 %) and 20 lpm (MARGA and RH 29 %). CIMS  
 7 (blue markers) and CI-Api-TOF (red markers) have been tested with 6 lpm and 10 lpm  
 8 (nominal) inlet total flowrates and also with an extra 1 m Teflon tubing after saturator.

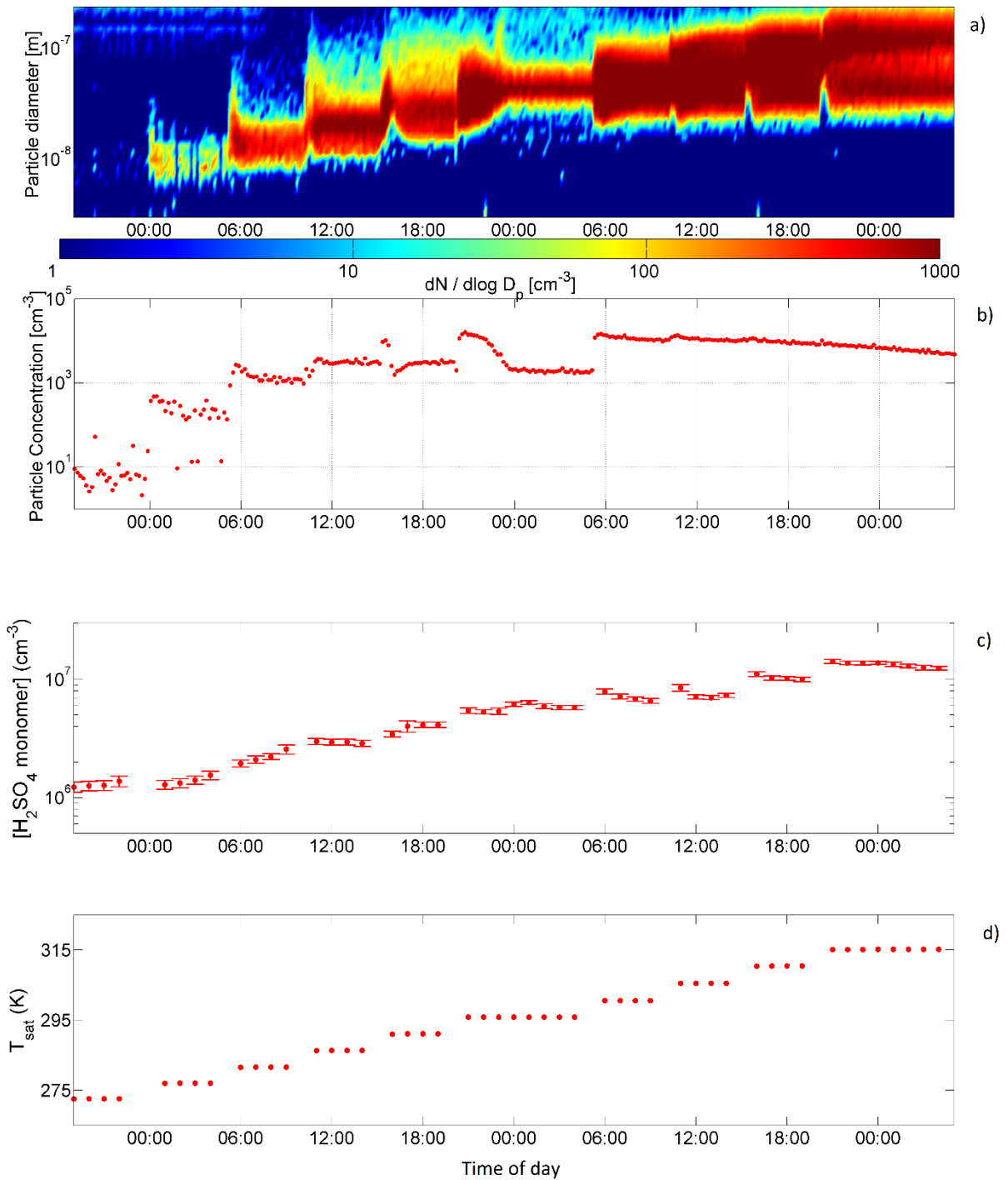




1

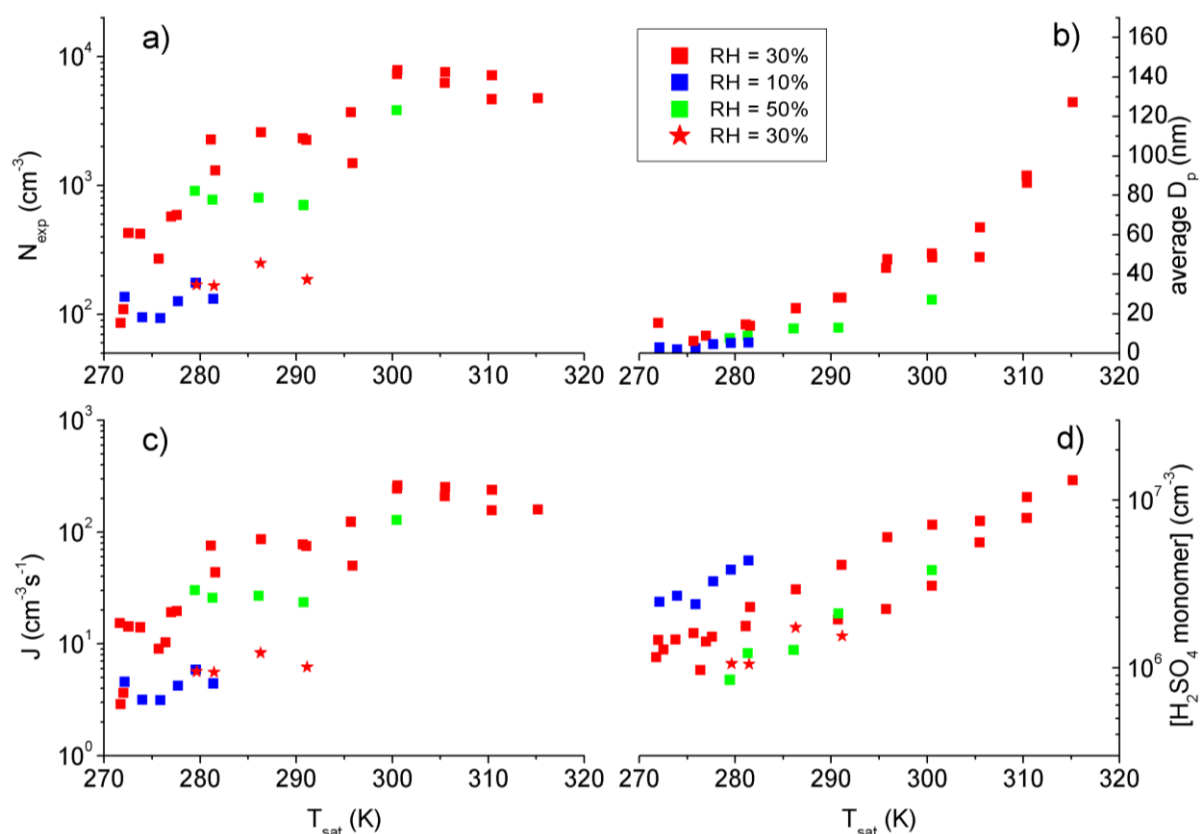
2

3 Figure 4. Comparison of MARGA and CIMS data between test with only saturator (dry  
 4 conditions, squares) and with saturator and flow tube (RH ~30 %, stars). Different flowrates  
 5 through saturator have been accounted for. Average total loss factors are  $TLF_{\text{MARGA}} = 10.0 \pm$   
 6  $1.2$  and  $TLF_{\text{CIMS}} = 14.2 \pm 4.2$ . See text for details.

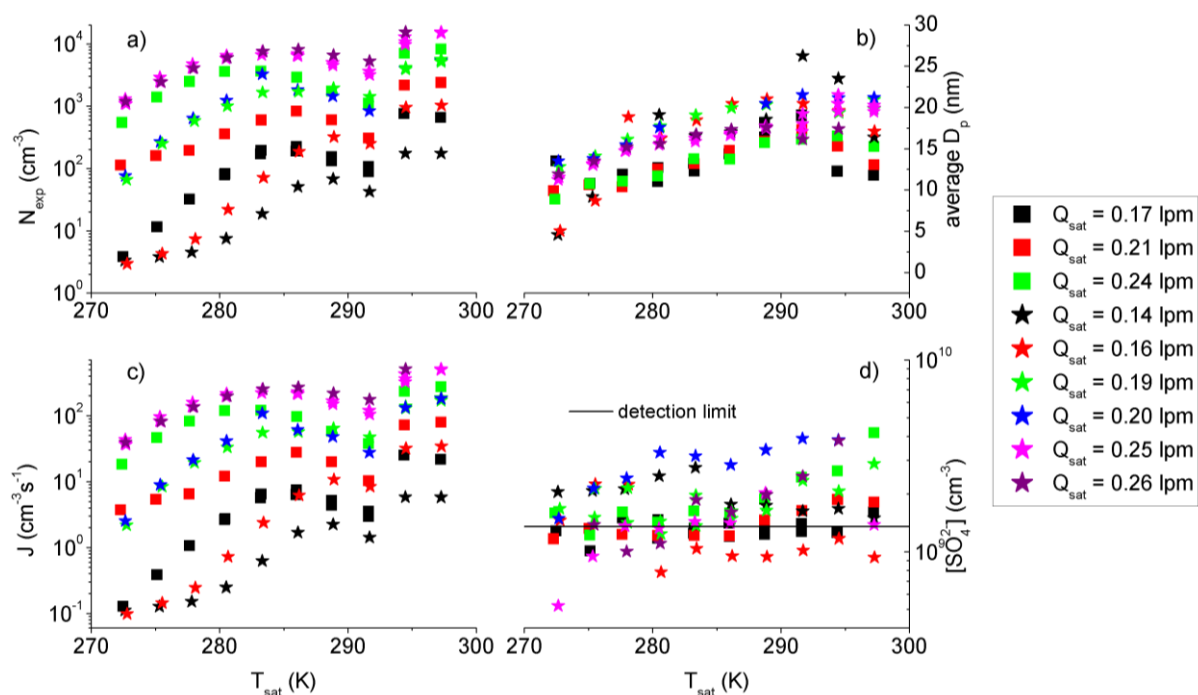


1  
2

3 Figure 5. DMPS and CIMS data from one  $T_{\text{sat}}$  cycle. Panel a) shows the number size  
4 distribution, panel b) shows the total number concentration from DMPS, panel c) shows the  
5 CIMS-measured sulphuric-acid monomer concentration averaged over one hour with standard  
6 deviation as error bars and panel d) shows hourly averaged temperature of the saturator.



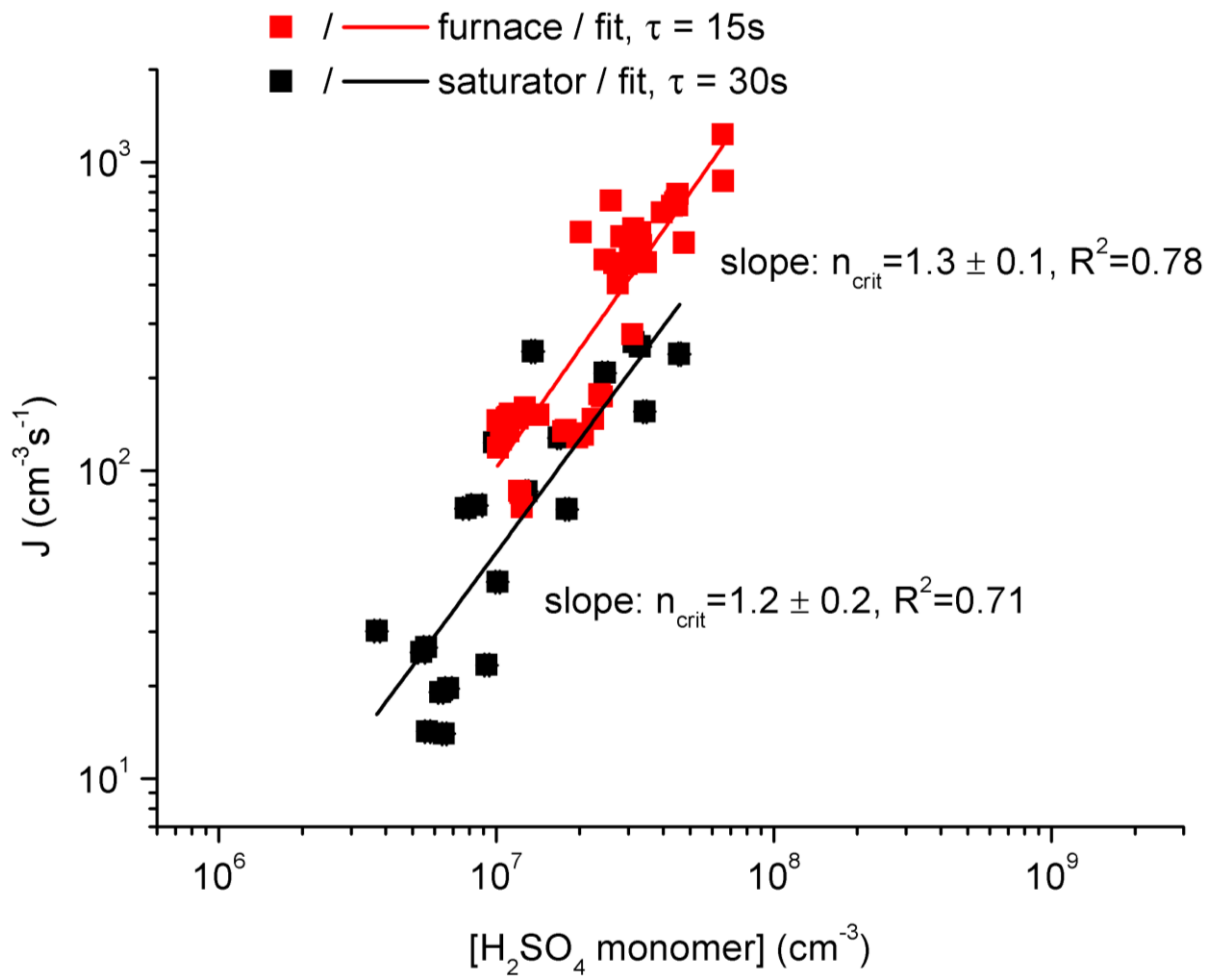
1  
 2  
 3 Figure 6. Number concentration  $N_{\text{exp}}$  (panel a)) measured with PSM and TSI 3776, geometric-  
 4 mean diameter  $D_p$  (panel b)), apparent formation rate  $J$  (panel c)) of the freshly nucleated  
 5 particles and sulphuric-acid monomer concentration measured (panel d)) with CIMS (squares)  
 6 or CI-Api-TOF (stars) with several relative humidity as a function of saturator temperature with  
 7 saturator flow of 0.1 lpm. All data are averaged over a period of constant saturator temperature  
 8 excluding first hour to ensure steady-state. Stars are measured with CI-Api-TOF and squares  
 9 with CIMS. All data are averaged over a period of constant saturator temperature ( $\pm 0.05$  K)  
 10 extracting first hour.



1

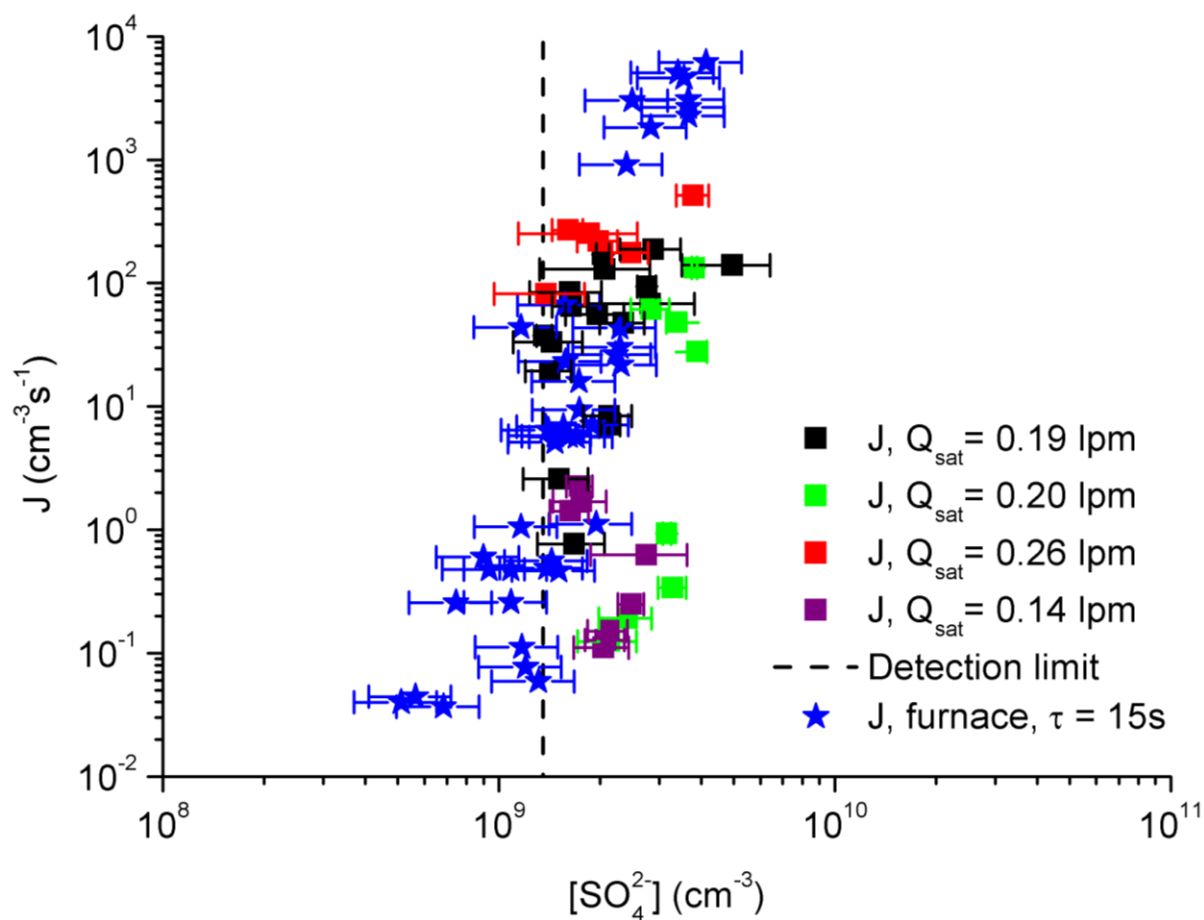
2

3 Figure 7. Number concentration  $N_{\text{exp}}$  (panel a)) measured with TSI 3776, geometric mean  
 4 diameter  $D_p$  (panel b)), formation rate  $J$  (panel c)) of the freshly nucleated particles and total-  
 5 sulphate concentration from MARGA (panel d)) with detection limit of MARGA with several  
 6 different saturator flowrates as a function of saturator temperature. Squares represent  
 7 measurements at dry conditions, stars are measured with  $\text{RH}$  of  $\sim 30\%$ . All data are averaged  
 8 over a period of constant saturator temperature ( $\pm 0.05$  K) extracting first hour.



1  
2

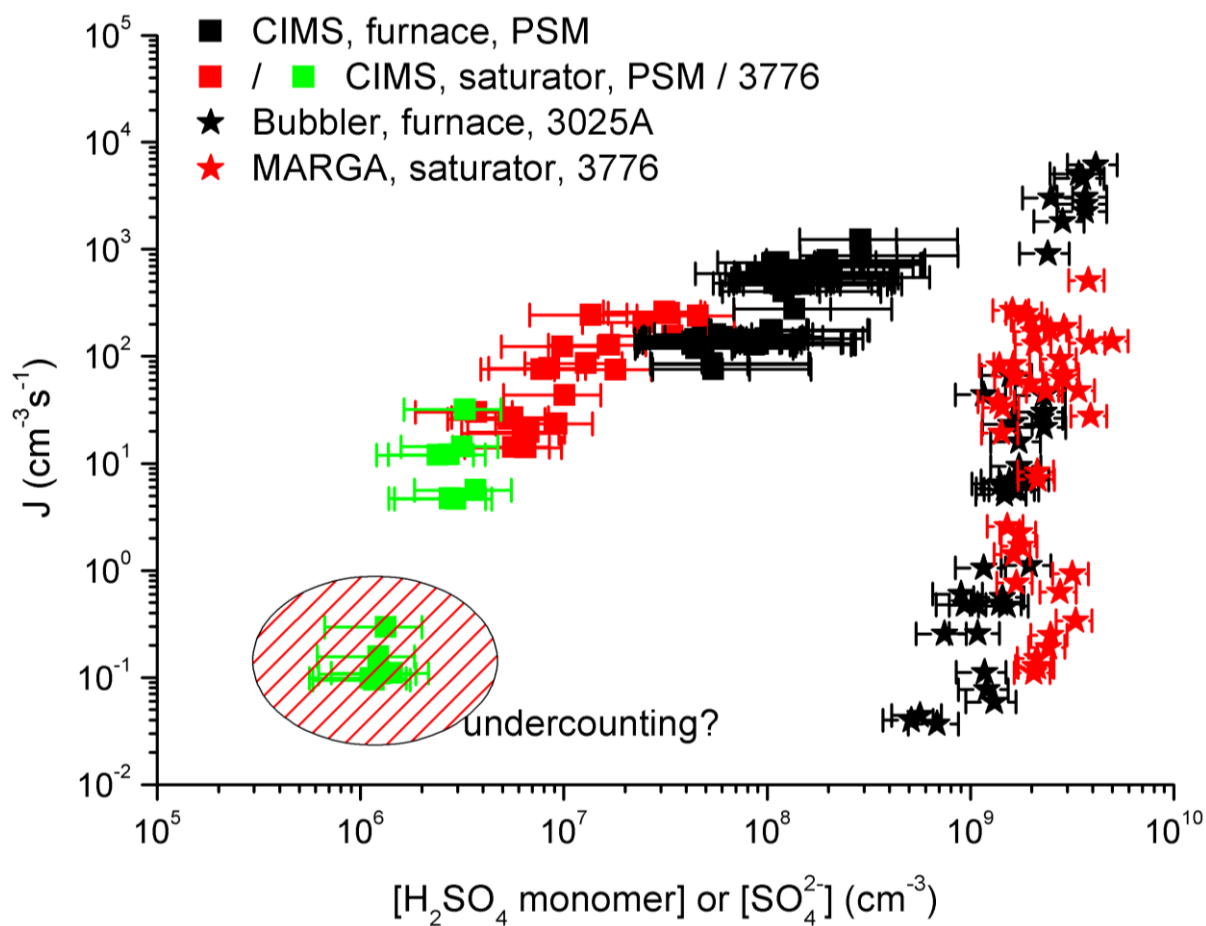
3 Figure 8. Formation rates  $J$  as a function of residual sulphuric acid monomer concentration  
 4  $[\text{H}_2\text{SO}_4 \text{ monomer}]$  at  $T = 298 \text{ K}$  and  $\text{RH} \sim 30 \%$  measured using CIMS. In the first dataset  
 5 (red squares) sulphuric-acid vapour was produced with the furnace method and the residence  
 6 time was defined to be 15 s (Brus et al., 2011).



1

2

3 Figure 9. Formation rates  $J$  as a function of total-sulphate concentration  $[SO_4^{2-}]$  measured  
 4 with MARGA or bubbler with different saturator flowrates. MARGA's detection limit is  
 5 marked with the dashed line. Relative humidity RH  $\sim$ 30 % and nucleation temperature  $T =$   
 6 298 K. Sulphuric-acid vapour was produced with the furnace method (Brus et al., 2010) for  
 7 bubbler measurements and with the saturator method for MARGA.



1

2

3 Figure 10. Comparison of formation rates  $J$  as a function of residual sulphuric-acid monomer  
 4 concentration  $[\text{H}_2\text{SO}_4]$  or total-sulphate concentration  $[\text{SO}_4^{2-}]$  to our previous results.  
 5 Conditions are similar ( $T = 298 \text{ K}$ ,  $\text{RH} \sim 30 \%$ ). Note the factor-of-two difference between the  
 6 residence times between furnace and saturator measurements. Sulphuric-acid vapour was  
 7 previously produced with the furnace method and total sulphate concentration measured with  
 8 the bubbler method (Brus et al., 2010).